

Dottorato in Fisica, Roma 3
Laboratori Nazionali di Frascati
13 - 14 giugno, 2016

High Brightness Photo-Injectors

Enrica Chiadroni
INFN - LNF

Outline

- Applications of electron sources
 - FEL, ERL, Inverse Compton scattering, THz sources, plasma-based accelerators
- Electron source figure of merit
 - Brightness
- Electron photo-injectors
 - Cathode physics
 - RF guns
 - Space charge effects
 - Emittance compensation
 - Injection into the linac
 - Acceleration and compression

Motivation

Free Electron Lasers (FELs), Energy Recovery Linacs (ERLs) light sources, Plasma-based accelerators, etc. demand

- *medium/high average current: from $\sim\mu\text{A}$ to mA and higher*
- *high brightness electron beams (HBEBs)*
 - ultra-low normalized emittance: $\sim\text{mm mrad}$ and less
 - high peak current: $\sim\text{kA}$
 - beam charge from few pC to 1 nC
 - Careful definition and specific requirements for both electron sources and injection systems
 - The final beam quality is set by the linac and ultimately by its injector and electron source

A large number of quasi-“monochromatic” electrons, concentrated in very short bunches, with small transverse size and divergence, means high particle density 6D phase-space **=> high brightness**

Brightness

1939 von Borries and Ruska (Nobel prize in Physics in 1986 for the invention of the Electron Microscope) introduced the so called beam brightness (“Richstrahlwert”) defined as:

$$B_{micr} = \frac{I}{A\Omega} \approx constant$$

The smaller the spot the larger the divergence.

The brightness defines then the quality of the source and determines the kind of experiments

$$Brightness = \frac{\text{Contrast}}{\underbrace{\pi r^2}_{\text{Spatial resolution}} \underbrace{\pi \alpha^2}_{\text{Coherence}} \underbrace{\Delta t}_{\text{Time resolution}}} Ne$$

5D Brightness

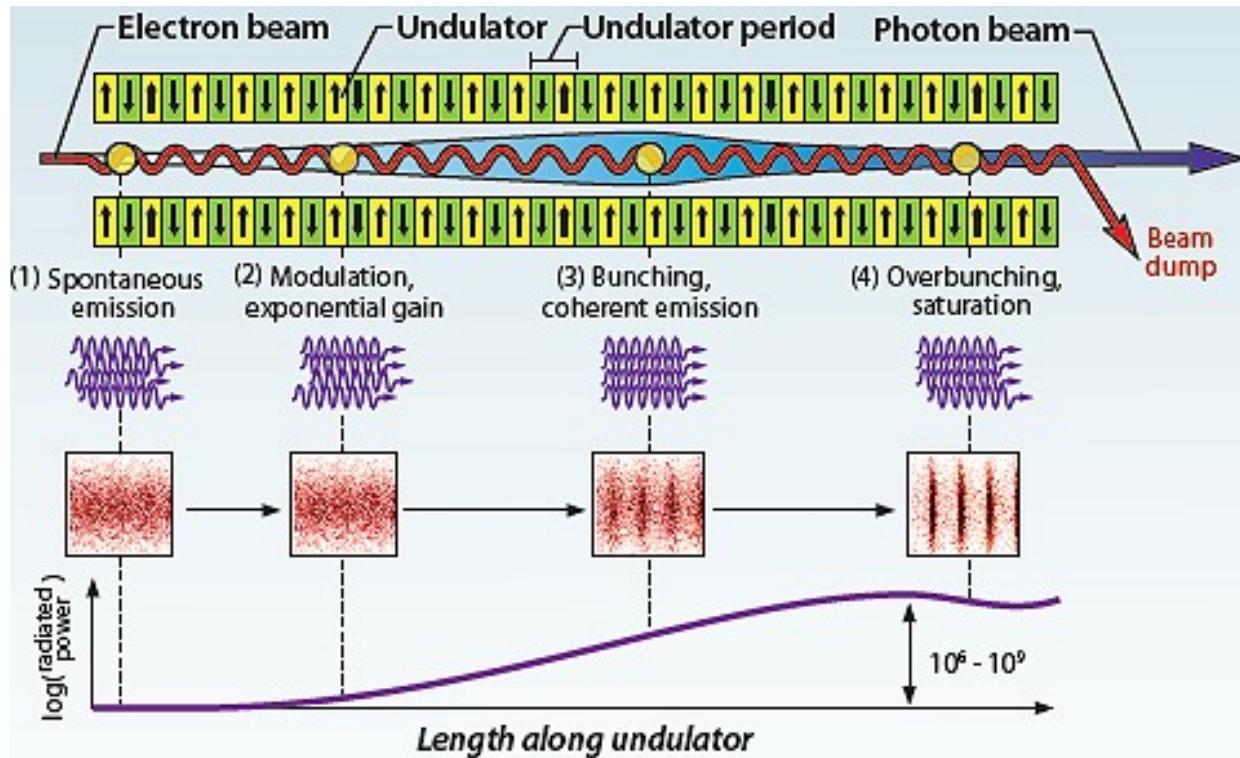
For FEL applications the 5D brightness is often used to compare electron sources

$$B_{5D} = \frac{2I}{\varepsilon_{nx}\varepsilon_{ny}} = \frac{2I}{(\beta\gamma)^2\varepsilon_x\varepsilon_y}$$

and it is the relativistic analogue of the microscopic brightness.

Pierce parameter

$$\rho = \frac{1}{2\gamma} \left[\frac{I}{I_A} \left(\frac{\lambda_u K [JJ]}{\sqrt{8\pi\sigma_x}} \right)^2 \right]^{1/3}$$



5D Brightness

For FEL applications the 5D brightness is often used to compare electron sources

$$B_{5D} = \frac{2I}{\varepsilon_{nx}\varepsilon_{ny}} = \frac{2I}{(\beta\gamma)^2\varepsilon_x\varepsilon_y}$$

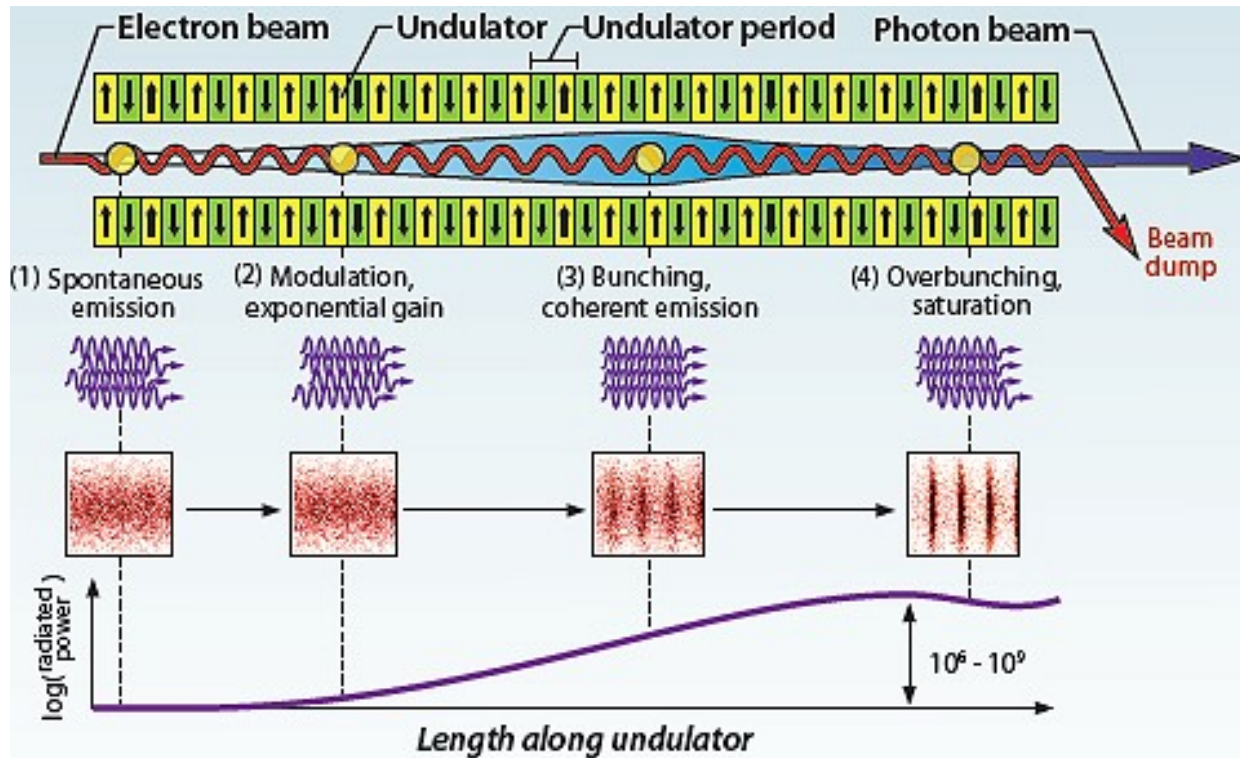
and it is the relativistic analog of the microscopic brightness.

Pierce parameter

$$\rho = \frac{1}{2\gamma} \left[\frac{I}{I_A} \left(\frac{\lambda_u K [JJ]}{\sqrt{8\pi\sigma_x}} \right)^2 \right]^{1/3}$$

Gain length

$$L_g = \frac{\lambda_u}{4\sqrt{3\pi\rho}}$$

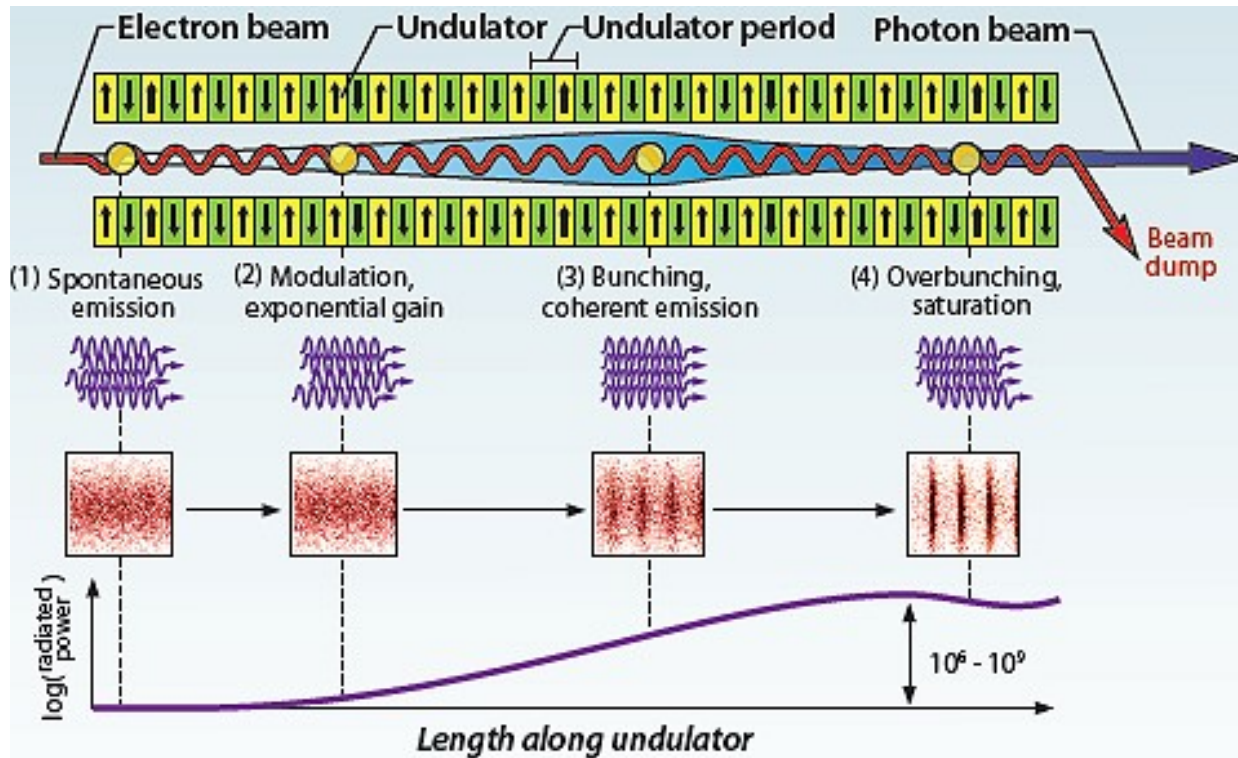


5D Brightness

For FEL applications the 5D brightness is often used to compare electron sources

$$B_{5D} = \frac{2I}{\varepsilon_{nx}\varepsilon_{ny}} = \frac{2I}{(\beta\gamma)^2\varepsilon_x\varepsilon_y}$$

and it is the relativistic analog of the microscopic brightness.



Pierce parameter

$$\rho = \frac{1}{2\gamma} \left[\frac{I}{I_A} \left(\frac{\lambda_u K [JJ]}{\sqrt{8\pi\sigma_x}} \right)^2 \right]^{1/3}$$

Gain length

$$L_g = \frac{\lambda_u}{4\sqrt{3}\pi\rho}$$

Saturation power

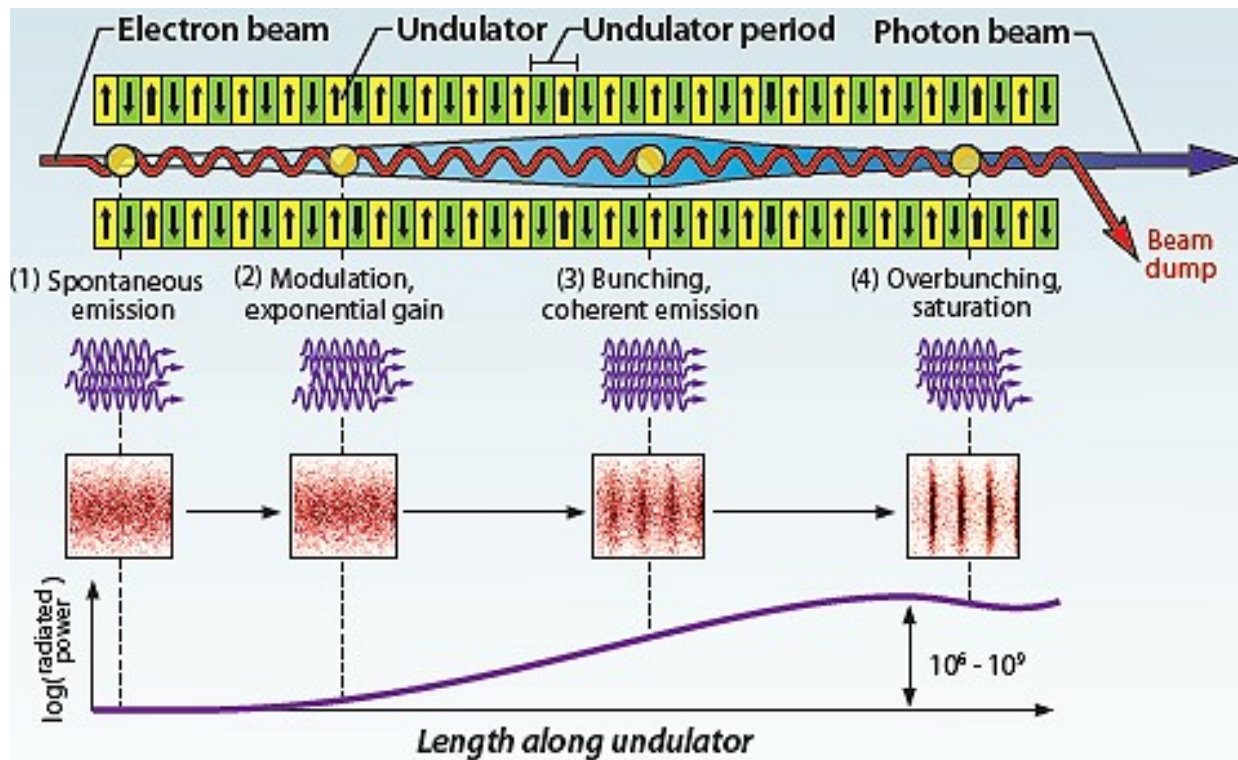
$$P = P_{in} e^{\frac{z}{L_g}}$$

5D Brightness

For FEL applications the 5D brightness is often used to compare electron sources

$$B_{5D} = \frac{2I}{\varepsilon_{nx}\varepsilon_{ny}} = \frac{2I}{(\beta\gamma)^2\varepsilon_x\varepsilon_y}$$

and it is the relativistic analog of the microscopic brightness.



Pierce parameter

$$\rho = \frac{1}{2\gamma} \left[\frac{I}{I_A} \left(\frac{\lambda_u K [JJ]}{\sqrt{8\pi\sigma_x}} \right)^2 \right]^{1/3}$$

Gain length

$$L_g = \frac{\lambda_u}{4\sqrt{3}\pi\rho}$$

Saturation power

$$P = P_{in} e^{\frac{z}{L_g}}$$

$$L_g \propto B_{5D}^{-\frac{1}{3}}$$

6D Beam Brightness

The meaningful figure of merit used to describe electron sources should be the 6D beam brightness defined as

$$B_{6D} = \frac{Ne}{V_{6D}}$$

where V_{6D} is the volume occupied by the beam in the 6D phase space (x, p_x, y, p_y, z, p_z)

$$V_{6D} = \int \psi(x, p_x, y, p_y, z, p_z) dx dp_x dy dp_y z dp_z$$

which is proportional to the product of the three normalized emittances

$$B_{6D} \propto \frac{Ne}{\epsilon_{nx} \epsilon_{ny} \epsilon_{nz}}$$

Liouville Theorem

The 6D phase space of non-interacting particles in a conservative dynamical system is invariant -> **Liouville theorem**

As long as the particle dynamics in the beamline elements (transport optics, accelerating sections) can be described by Hamiltonian functions (no binary collisions, stochastic processes, etc.), the phase space density will stay constant throughout the accelerator.

The 6D brightness of a beam is determined by the source and cannot be improved, but only spoiled along the downstream accelerator.

The brightness generated at the electron source represents the ultimate value

Possible sources of rms emittance growth

Non-linear space charge forces

Non linear forces from electromagnetic components

Synchrotron radiation emission (in magnetic compressors)

Brightness Quantum Limit

Due to the *Pauli exclusion principle*, there is a **maximum brightness theoretically achievable** by an electron beam, as the 6D phase space density is fundamentally limited, with one electron spin up-down pair in each elementary quantum h^3 unit of phase space volume, as set by *Heisenberg uncertainty principle*

$$B_{\text{quantum}} = \frac{2e}{h^3} (m_0 c)^3 = \frac{2e}{\lambda_c^3} \approx 10^{25} \frac{A}{m^2}$$

The degeneracy parameter δ represents the number of particles per elementary volume of the phase space

$$\delta = \frac{B}{B_{\text{quantum}}}$$

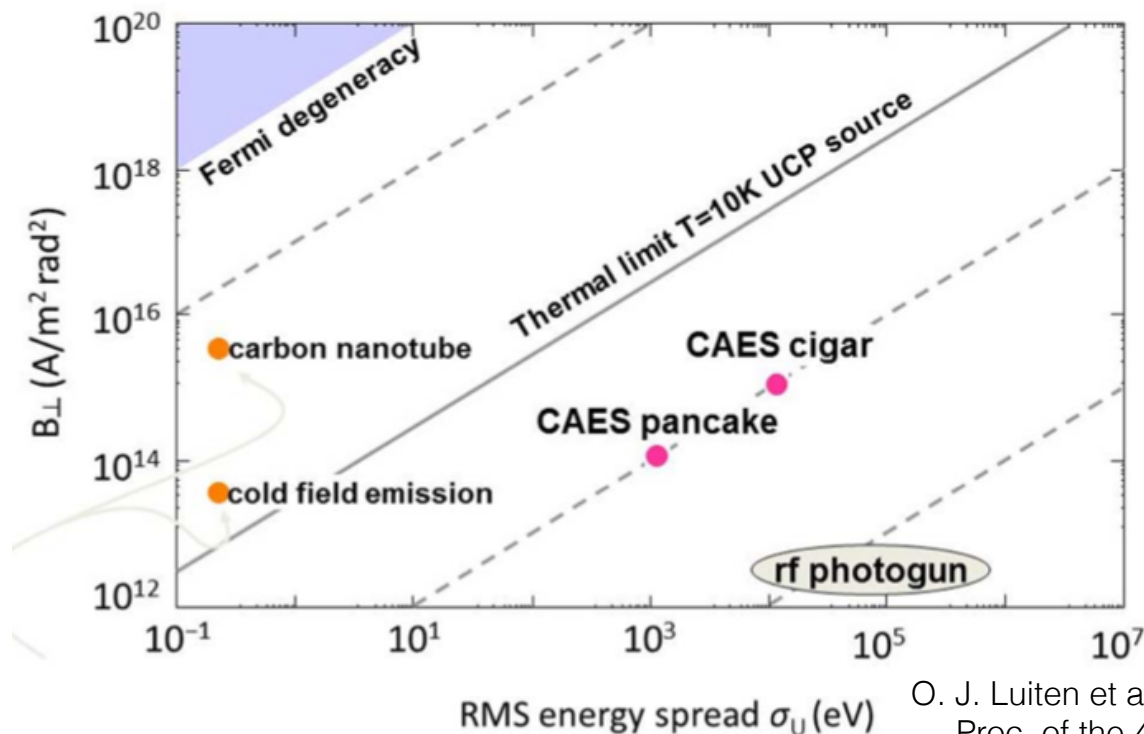
State-of-the-art electron sources

In numbers: $N \approx 10^9$, $\sigma_\gamma \approx 10^{-3}$, $\varepsilon_n \approx 1 \text{ mm mrad}$, $\sigma_t \lesssim 1 \text{ ps}$

$$B \approx 10^{15} \frac{A}{m^2}$$

Brightness Quantum Limit

$$B_{6D} \propto \frac{Ne}{\epsilon_{nx}\epsilon_{ny}\sigma_t\sigma_\gamma}$$



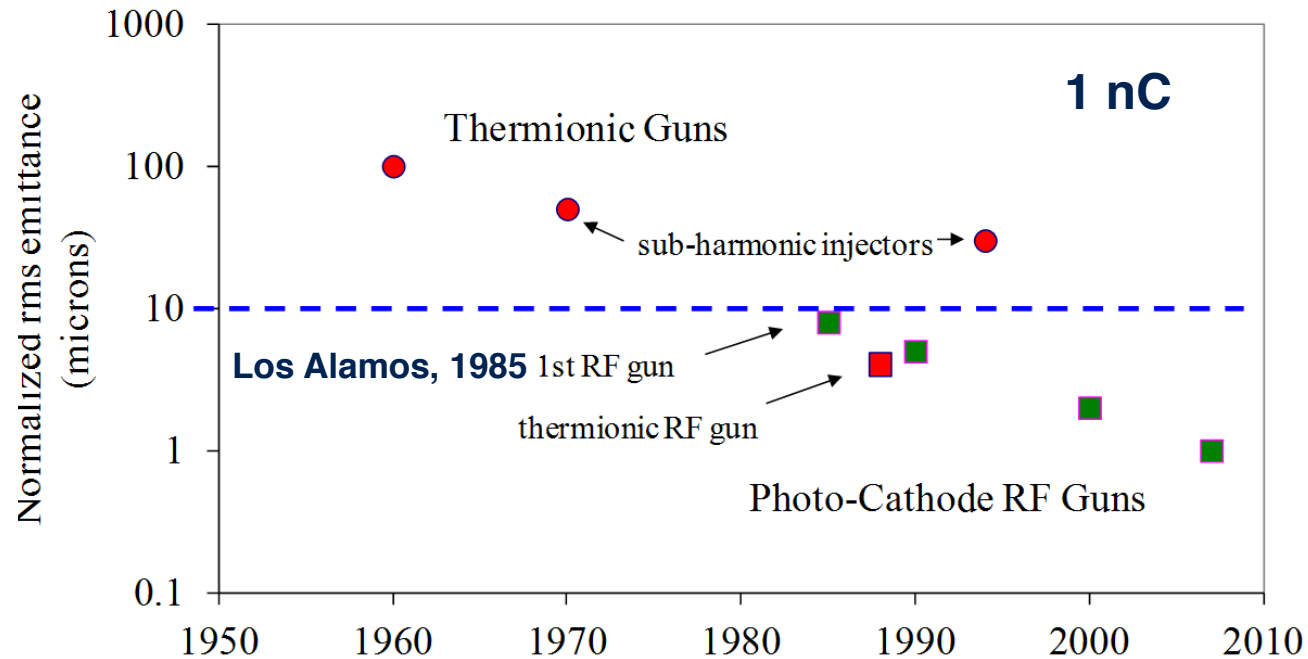
O. J. Luiten et al., Ultracold electron sources,
Proc. of the 46th Workshop of the INFN
Eloisatron Project, Erice 2005

The degeneracy factor inside a metal is ~ 1 .

How do we lose 10^{-11} orders of magnitude then?

Electron emission mechanism and Coulomb interaction

Injectors: a bit of history



Dowell, Rao, *An Engineering Guide To Photoinjectors*,

The **need for fast and precise control of the electron pulse shape** for better beam quality led to the replacement of thermionic gun with **photocathode RF guns** because of the impressive reduction in transverse emittance (10 times and more), promoted by the **ability to shape drive laser pulses and rapidly accelerate electrons from rest to relativistic energies**

Elements of an Electron Injector

- An **electron injector** is the **first part of the accelerating chain**
 - The **electron beam generated at rest energy** is accelerated and **guided up to** energies where space charge force effects are negligible and under control, therefore **its evolution is not space charge dominated anymore**
 - Space charge forces scale inversely with the square of the beam energy
- Space charge forces influence the beam dynamics and are one the main performance limitations in high brightness electron injectors

Emission and initial acceleration

- Thermionic cathode
 - DC gun
 - NCRF gun
- Photo-electric cathode
 - DC gun
 - NCRF gun
 - SCRF gun
- Field emission cathode
 - Pulse-DC
 - RF

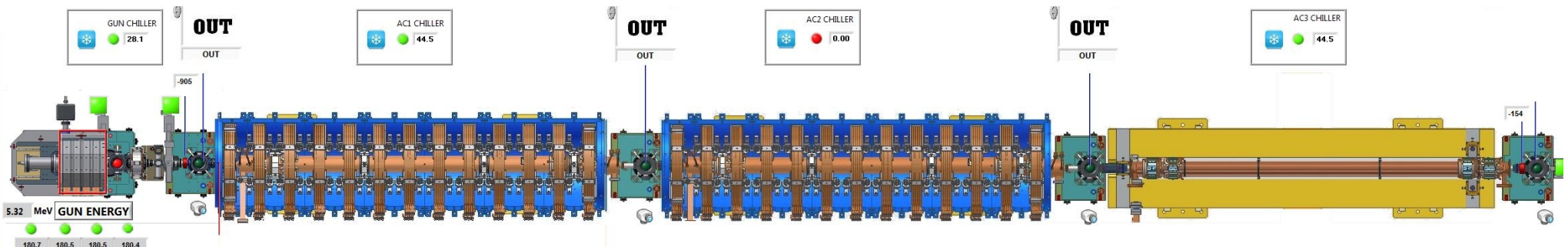
Beam manipulation

- Emittance compensation
 - Solenoid focusing
 - RF focusing
 - Slice phase space matching
- Ballistic compression
 - ...
- Magnetic compression
 - RF harmonic linearization
- RF compression
 - Solenoid focusing

Acceleration

- Capture into the booster
- Emittance preservation
- Longitudinal phase space preservation

Elements of an Electron Injector



Emission and initial acceleration

- Thermionic cathode
 - DC gun
 - NCRF gun
- **Photo-electric cathode**
 - DC gun
 - **Normal Conducting RF gun**
 - SCRF gun
- Field emission cathode
 - Pulse-DC
 - RF

Beam manipulation

- **Emittance compensation**
 - Solenoid focusing
 - RF focusing
 - Slice phase space matching
- Ballistic compression
 - ...
- **Magnetic compression**
 - RF harmonic linearization
- **RF compression**
 - Solenoid focusing

Acceleration

- Capture into the booster
- Emittance preservation
- Longitudinal phase space preservation

High Brightness Photo-injector Components

A **photo-injector** consists of a **laser generated electron source** followed by an electron beam optical system which preserves and matches the beam into a high-energy accelerator

- **Drive laser**
 - To gate the emission of electrons from the cathode
- **Photocathode**
 - Releases picosecond electron bunches when irradiated with laser pulses
- **Electron Gun**
 - Accelerates electrons from the rest
 - The high electric fields produced by rf guns are necessary both to extract the high currents and to minimize the effects of space charge on emittance growth while the bunch is accelerated to relativistic energies where the space-charge forces vanish
 - Acts as strong defocusing lens => **Solenoid magnet**
- **Accelerating system**
 - to mitigate the space charge emittance growth

Typical High Brightness Photo-injector Layout

A typical photocathode RF system depicts a 1½-cell gun with a cathode in the ½ cavity being illuminated by a laser pulse train. At the exit of the gun is a solenoid which focuses the divergent beam from the gun and compensates for space charge emittance. The drive laser is mode-locked to the RF master oscillator which also provides the RF drive to the klystron.

RF frequencies

- 1.3 GHz: L-band
- 2.856 GHz: S-band
- 5.6 GHz: C-band
- 11- 17 GHz X-band

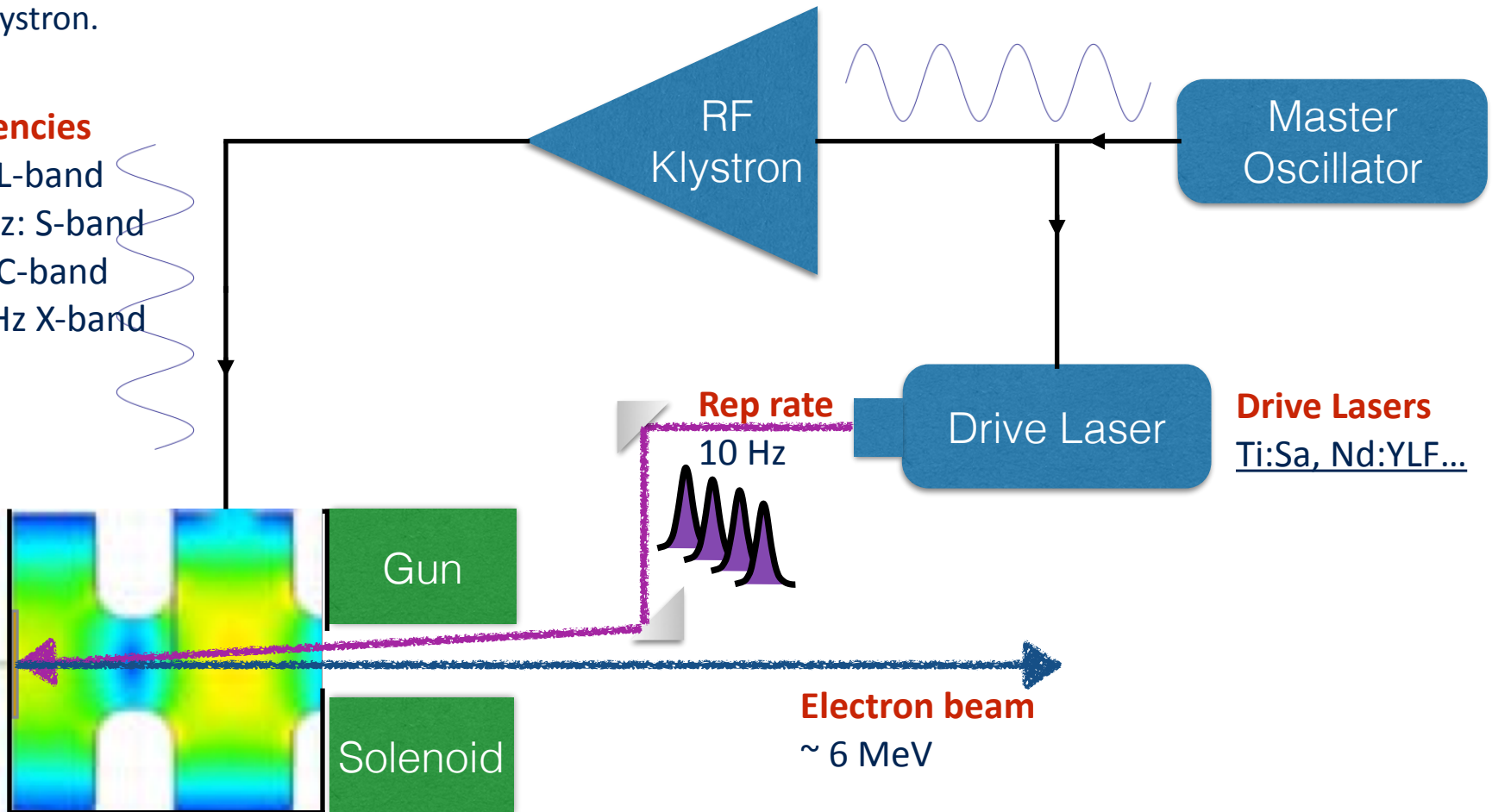


Photo-cathodes

Metal: Cu, Mg, ...

Semi-conductor: CsTe, CsKSb, ...

Cathode physics

- Cathodes are a fundamental part of electron sources
- Most injector systems use photocathodes
 - Exception: SACLA XFEL which uses a thermionic cathode
- The ideal cathode should have **low intrinsic emittance, high quantum efficiency, long life-time, uniform emission** and should allow for low energy spread, high current density beams and full control of bunch distribution => **fast response**
- Low charge regime: the ultimate brightness performance of the linac is set by the **cathode intrinsic emittance**
- High repetition rates photon sources: high **quantum efficiency** photocathodes are required

Electron emission

The **emission process determines the fundamental lower limit of the beam emittance**, called as **intrinsic emittance**, which depends on the three emission mechanisms

1. **thermionic** emission
2. **field** emission
3. **photo-electric** emission

The probability of a particle to occupy a given energy state is described by a proper statistic.

Particles which can share the same energy state follow the **Maxwell-Boltzmann (MB) distribution**,

$$f_{MB} = e^{-E/k_B T}$$

while those having only one particle per energy state follow the **Fermi-Dirac (FD) distribution**

$$f_{FD} = \frac{1}{1 + e^{(E-E_F)/k_B T}}$$

The MB distribution is used for thermionic emission, while **field and photo-emission** calculations use the FD distribution, since the excited **electrons come from energy levels below the Fermi level, i.e. $E < E_F$**

Fields near the cathode surface

Electric potential energy

$$e\Phi_{tot} = e\Phi_{work} - \frac{e^2}{16\pi\epsilon_0 x} - eE_0x$$

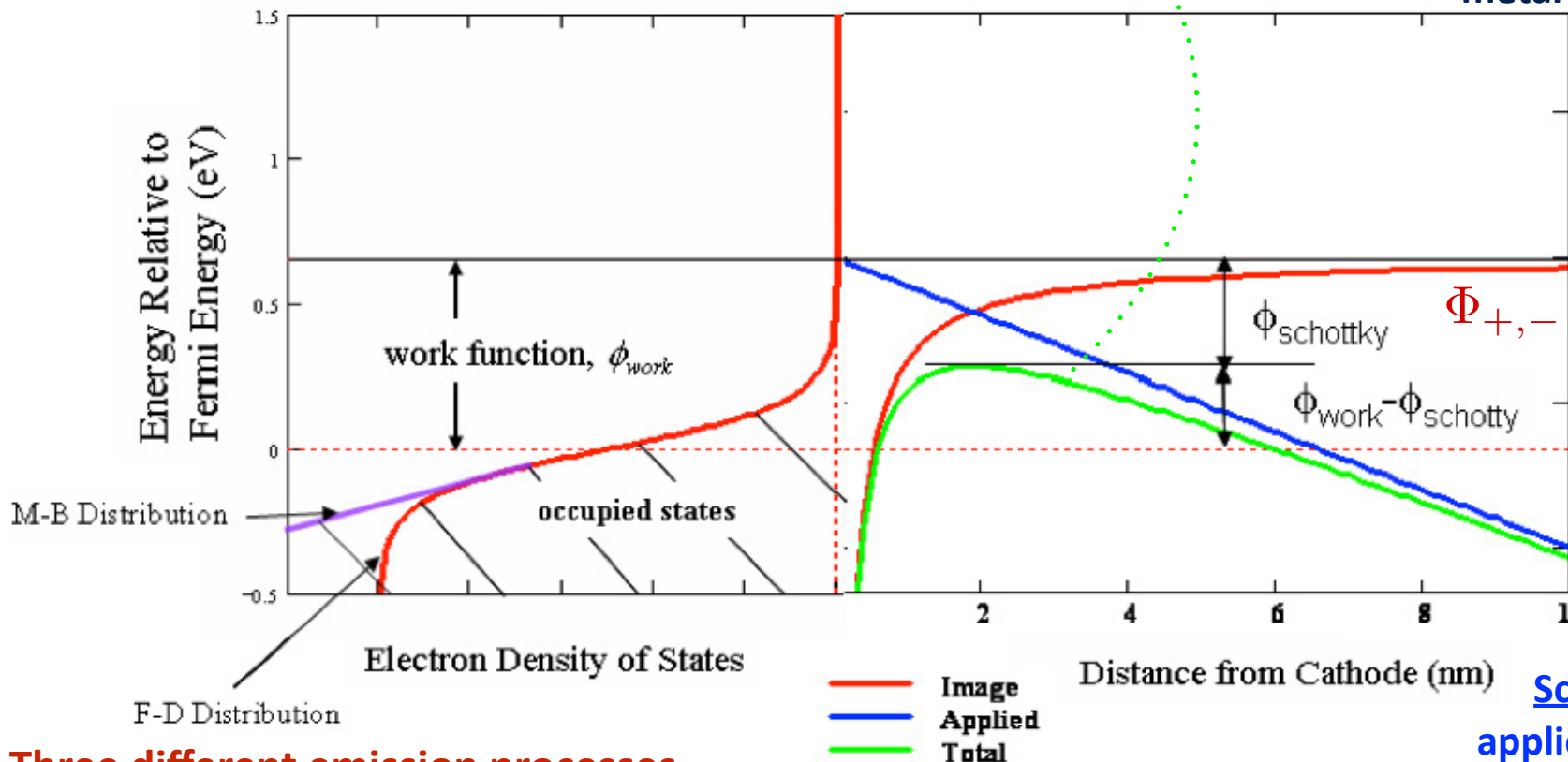
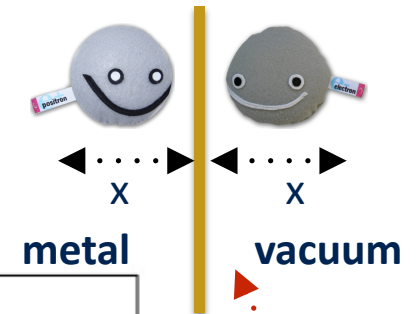


Image charge

$$\Phi_{+,-} = -\frac{e^2}{16\pi\epsilon_0 x}$$

Schottky effect

applied external field
lower the barrier

$$\Phi_{sh} = -eE_0x$$

Three different emission processes

1. Thermionic emission → Require electrons with energies greater than the work function to escape the barrier
2. Photo-electric emission → Require electrons with energies greater than the work function to escape the barrier
3. Field emission → Consequence of the Schottky effect. Electrons tunneling the barrier. Very fast dependence on applied field => **DARK CURRENT**

Photo-electric Emission

Spicer's three-step photoemission model

1. Photon energy absorption by electron

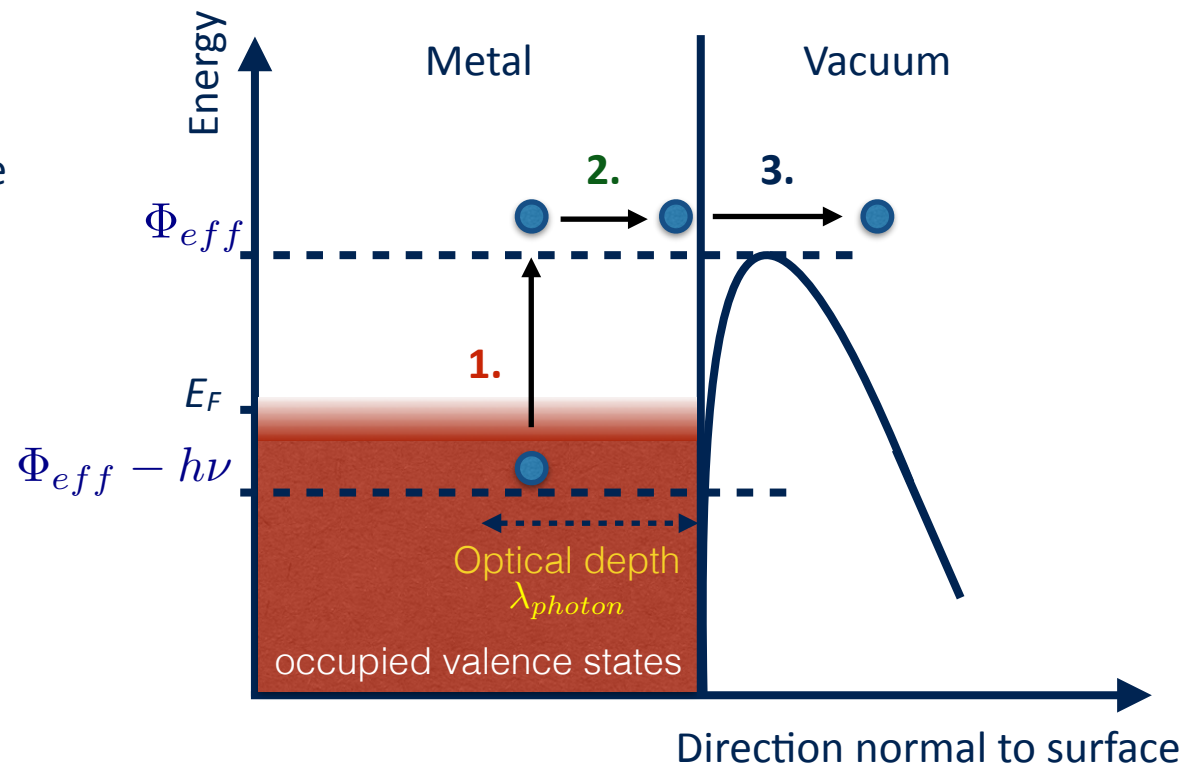
- The optical skin depth depends on photon wavelength (~ 14 nm for UV light on Cu)
 - reflectivity and absorption as the photons travel into the cathode

2. electron transport to the surface

- electron-electron scattering
- electron-phonon scattering
- angular cone of escaping electrons

3. electron escape through the barrier

- Schottky effect and abrupt change in electron angle across the metal-vacuum interface
- classical escape over the barrier due to the applied field



Quantum Efficiency

Combining the three steps together, the quantum efficiency, QE, can be expressed in terms of the probabilities for these processes to occur

1. absorption of the photon with energy $\hbar\omega$
2. migration including e-e scattering to the surface
3. escape for electrons with kinematics above the barrier

$$QE(\omega) = [1 - R(\omega)] F_{e-e}(\omega) \frac{\int_{E_F + \Phi_{eff} - \hbar\omega}^{E_F} dE \int_{-1}^1 \sqrt{\frac{E_F + \Phi_{eff}}{E + \hbar\omega}} d(\cos \vartheta) \int_0^{2\pi} d\phi}{\int_{E_F - \hbar\omega}^{E_F} dE \int_{-1}^1 d(\cos \vartheta) \int_0^{2\pi} d\phi}$$



Probability of a photon to be absorbed by the metal
=> **optical reflectivity**

$R(\omega) \sim 40\%$ for metals
 $R(\omega) \sim 10\%$ for semiconductors



Probability that an electron reaches the surface without scattering => **transport to surface**

e-e- scattering for metals
e-phonon scattering for semiconductors with another electron

$F_{e-e}(\omega) \sim 0.2$



Probability that an electron will be excited into a state with sufficient perpendicular momentum to escape the material => **escape over the barrier**

- occupied states with enough energy to escape ~ 0.04
- electrons with angle within the max angle for escape ~ 0.01
- azimuthally isotropic emission ~ 1

$$QE(\text{Cu}) \sim 0.6 * 0.2 * 0.04 * 0.01 * 1 \sim 5 * 10^{-5}$$

Quantum Efficiency

Combining the three steps together, the quantum efficiency, QE, can be expressed in terms of the probabilities for these processes to occur

1. absorption of the photon with energy $\hbar\omega$
2. migration including e-e scattering to the surface
3. escape for electrons with kinematics above the barrier

$$QE(\omega) = [1 - R(\omega)] F_{e-e}(\omega) \frac{\int_{E_F + \Phi_{eff} - \hbar\omega}^{E_F} dE \int_{-1}^1 \frac{d(\cos \vartheta)}{\sqrt{\frac{E_F + \Phi_{eff}}{E + \hbar\omega}}} \int_0^{2\pi} d\phi}{\int_{E_F - \hbar\omega}^{E_F} dE \int_{-1}^1 d(\cos \vartheta) \int_0^{2\pi} d\phi} \propto (\hbar\omega - \Phi_{eff})^2$$

Probability of a photon to be absorbed by the metal
=> **optical reflectivity**

$R(\omega) \sim 40\%$ for metals
 $R(\omega) \sim 10\%$ for semiconductors

Probability that an electron reaches the surface without scattering => **transport to surface**

e-e- scattering for metals
e-phonon scattering for semiconductors with another electron

$F_{e-e}(\omega) \sim 0.2$

Probability that an electron will be excited into a state with sufficient perpendicular momentum to escape the material => **escape over the barrier**

- occupied states with enough energy to escape ~ 0.04
- electrons with angle within the max angle for escape ~ 0.01
- azimuthally isotropic emission ~ 1

$$QE(\text{Cu}) \sim 0.6 * 0.2 * 0.04 * 0.01 * 1 \sim 5 * 10^{-5}$$

Intrinsic Emittance

The total energy inside the cathode after absorption of the photon is $E + \hbar\omega$, therefore the total momentum inside and outside is

$$p_{total,in} = \sqrt{2m(E + \hbar\omega)} \quad p_{total,out} = \sqrt{2m(E + \hbar\omega - \Phi_{eff} - E_F)}$$

The usual definition of rms emittance is

$$\epsilon_{n,x} = \beta\gamma \sqrt{\langle x^2 \rangle \langle x'^2 \rangle - \langle xx' \rangle^2} = 0, \text{ no correlation between angle and position of electrons out of the cathode}$$

σ_x transverse beam size determined by the size of the source, i.e. laser pulse

$$\epsilon_{n,x} = \sigma_x \frac{\sqrt{\langle p_x^2 \rangle}}{mc}$$

p_x transverse momentum determined by the emission process

$$\langle p_x^2 \rangle = \frac{\int \int \int p_x^2 g(E, \vartheta, \phi) dE d(\cos \vartheta) d\phi}{\int \int \int g(E, \vartheta, \phi) dE d(\cos \vartheta) d\phi}$$

$g(E, \vartheta, \phi) = [1 - f_{FD}(E + \hbar\omega)] f_{FD}(E)$ electron distribution function which depends on the emission process

Photo-electric normalized emittance

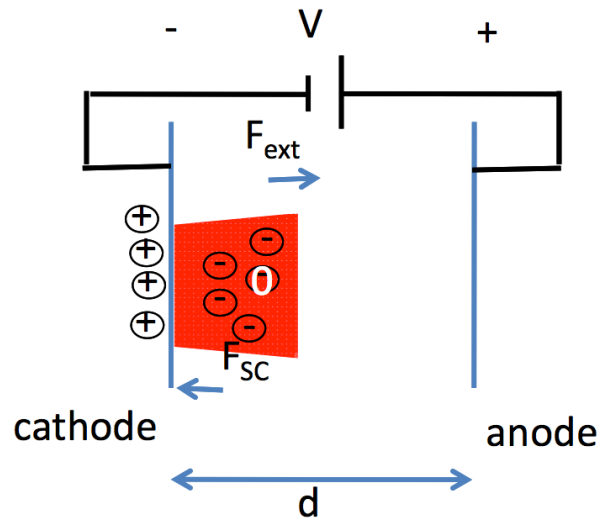
$$\epsilon_{n,x}^{intrinsic} = \sigma_x \sqrt{\frac{\hbar\omega - \Phi_{eff}}{3mc^2}}$$

Cu cathode

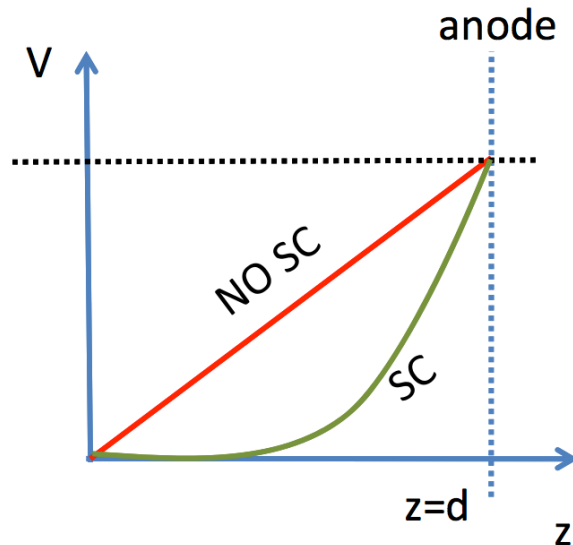
$$\approx 0.4 \text{ mm mrad/mm}$$

Space Charge Effects

As emitted particles come out from the cathode, they create their own electric field



As electrons are extracted they start to fill the entire region of length d



This field in the beam tail is opposed to the external field, growing with the extracted charge

The effective total potential is distorted by this field

- The potential distortion creates asymmetries in the electron beam (tails) and set a **maximum extractable current in the steady state regime**

Child-Langmuir Law

The maximum current density in an electron source is typically given by the Child-Langmuir law, expressing how the steady state current varies with both the gap distance and the bias potential of the parallel plates:

$$j_{CL,1D} = \frac{4\epsilon_0}{9} \sqrt{\frac{2e}{m}} \frac{V_0^{3/2}}{d^2}$$

Assumptions

- **infinitely wide beam** in the transverse dimensions (1D approximation)
- the **beam completely fills the accelerating gap** so that a steady state solution can be found
- **relativistic effects** can be **neglected**

BUT

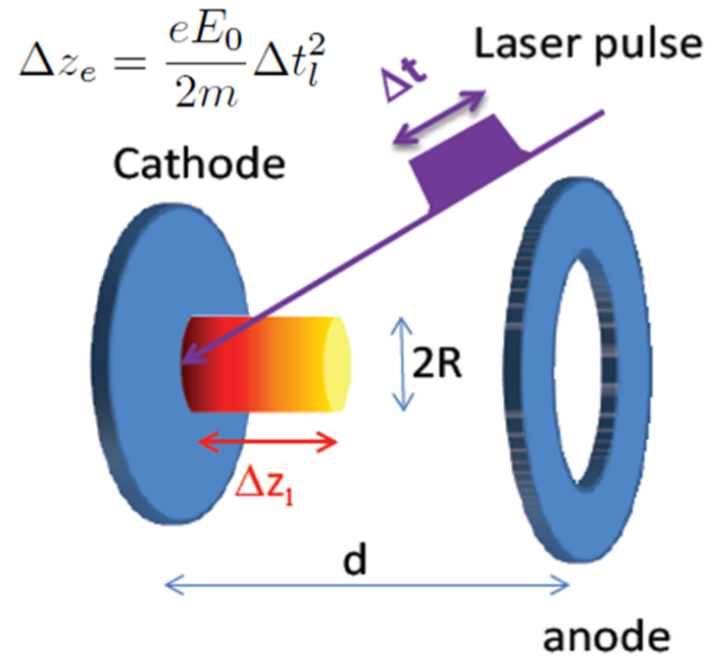
In state-of-art photo-injectors

- the initial **electron beam pulse length** is always much **smaller than the accelerating gap**
- the **laser spot size** on the cathode tends to be small (**sub-mm**) to decrease the cathode emittance contribution

The 1D Child-Langmuir formula is not valid anymore

Space Charge Limit

Let's consider short bunches and introduce the **aspect ratio**



$\frac{R}{\Delta z_e} \ll 1$ **cigar-like beams**

Only a small part of the beam contributes to the space charge field and higher charge can be extracted

$\frac{R}{\Delta z_e} \gg 1$ **pancake-like beams**

The maximum surface density is set by the cathode extraction field

$$Q = J_{CL} \pi R^2 \propto \frac{V^{\frac{3}{2}}}{d^2} R^2 \propto (E_0 R)^{\frac{3}{2}}$$

Courtesy of P. Musumeci

$$\frac{Q}{\pi R^2} < \epsilon_0 E_0$$

Space Charge Limit Emittance

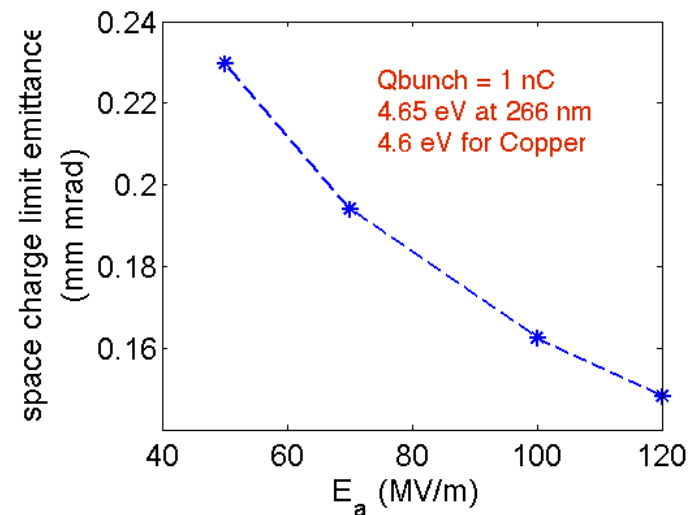
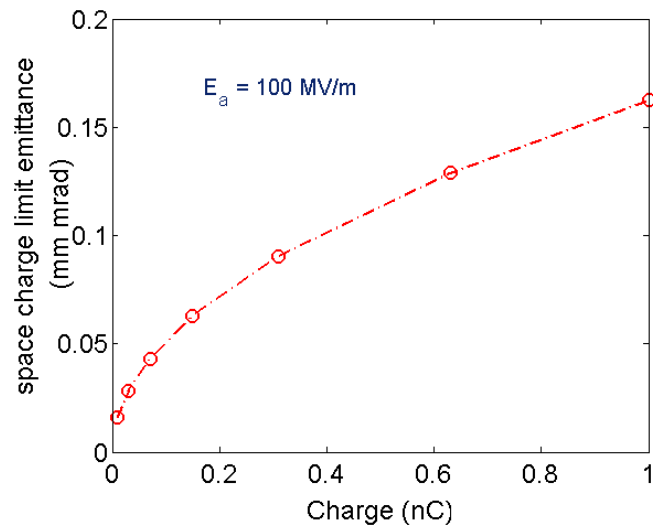
The SCL sets a minimum value for the beam emittance, once the applied field (RF field) value and the requested charge are known.

For a cylindrical uniformly filled beam with radius R, the rms size is

$$\sigma_x = \frac{R}{2} = \sqrt{\frac{Q_{bunch}}{4\pi\epsilon_0 E_a}}$$

Substituting the normalized divergence for photo-electric emission, σ_x' , the normalized cathode emittance results in the SCL photoelectric emittance

$$\epsilon_{photo}^{SCL} = \sqrt{\frac{Q_{bunch}(\hbar\omega - \Phi_{eff})}{4\pi\epsilon_0 mc^2 E_a}}$$



RF Gun

Since we wish to accelerate electrons, the relevant modes are those with large longitudinal electric fields, E_z

$$\frac{dU}{dt} = q\vec{v} \cdot \vec{E}$$

These are the transverse magnetic (TM) modes.

The TM_{mnp} designation denotes the mode is transverse magnetic since $B_z = 0$

m mode number: azimuth angle, ϑ -dependence or rotational symmetry of the fields $\Rightarrow m = 0$ for all RF guns, since a beam with rotational symmetry is desired

n mode number: radial dependence of the field

p mode number: longitudinal mode of cavity \Rightarrow RF emittance

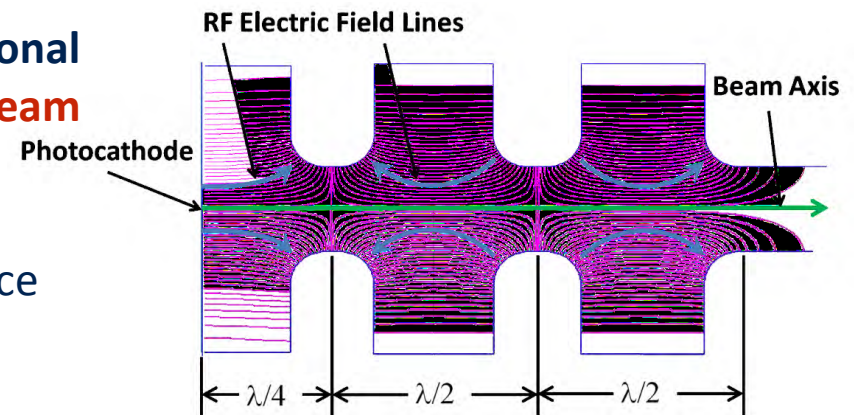
The full cell length for most RF guns is $\lambda/2$ and $p = 1$.

The longitudinal electric field for a pill box cavity is

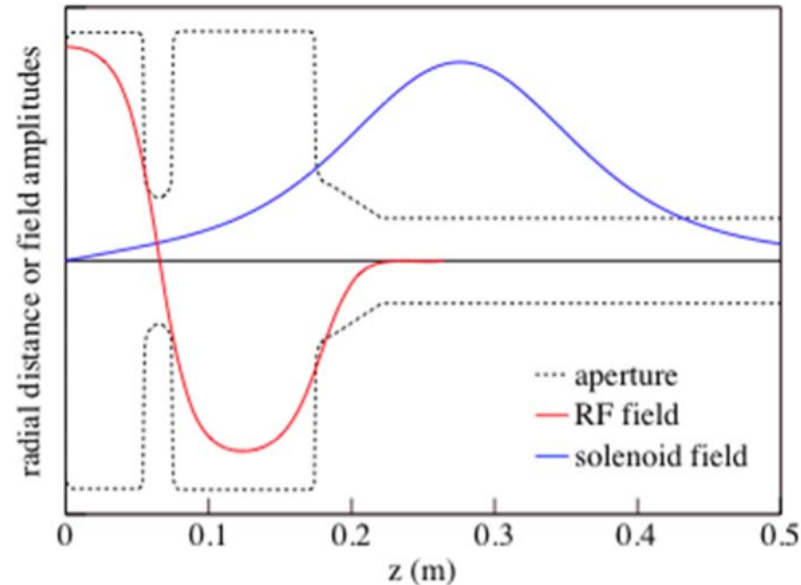
$$E_z^{mnp}(r, z) = E_0 J_m(k_{mn}r) \cos(m\theta) \cos\left(\frac{2p\pi z}{\lambda}\right) e^{i\omega \frac{z}{c}}$$

Consider the pi-mode for a one and a half cell gun, therefore $m=0, n=0, p=1$, then the gun field

$$E_z = E_0 \cos(kz) \sin(\omega t + \phi_0), \quad k = \frac{\omega}{c}$$



RF Gun



First order approximation from Maxwell equations solution for fundamental accelerating mode in a pillbox cavity.

Maxwell's equation **connect the momentum kicks of the radial electric field to the z- and t-derivative of the longitudinal electric field:**

$$E_z = E_0 \cos(kz) \sin(\omega t + \phi_0)$$

$$E_r = \frac{kr}{2} E_0 \sin(kz) \sin(\omega t + \phi_0) = -\frac{r}{2} \frac{\partial}{\partial z} E_z$$

$$B_\theta = c \frac{kr}{2} E_0 \cos(kz) \cos(\omega t + \phi_0) = \frac{r}{2c} \frac{\partial}{\partial t} E_z$$

Radial force

$$F_r = e(E_r - \beta c B_\theta)$$

Optical properties of the gun RF field

The radial momentum kick is

$$\Delta p_r = e \int E_r \frac{dz}{\beta c} = -\frac{e}{2} \int \frac{r}{\beta c} \frac{\partial E_z}{\partial z} dz$$

If we assume that the RF field is a constant step function in over the gun length, and integrate the force impulse over the position at the exit iris, the change in radial momentum is obtained

$$\Delta p_r = -\frac{eE_0}{mc^2} r \sin \phi \quad (\phi = \omega t + \phi_0 - k_z z_f)$$

Moving from cylindrical to cartesian coordinates we obtain the change in transverse momentum at the exit of the iris in terms of a kick angle

$$\Delta p_x = \beta \gamma x' = -\frac{eE_0}{2mc^2} x \sin \phi \quad \rightarrow \quad x' = -\frac{eE_0}{2\beta \gamma mc^2} x \sin \phi$$

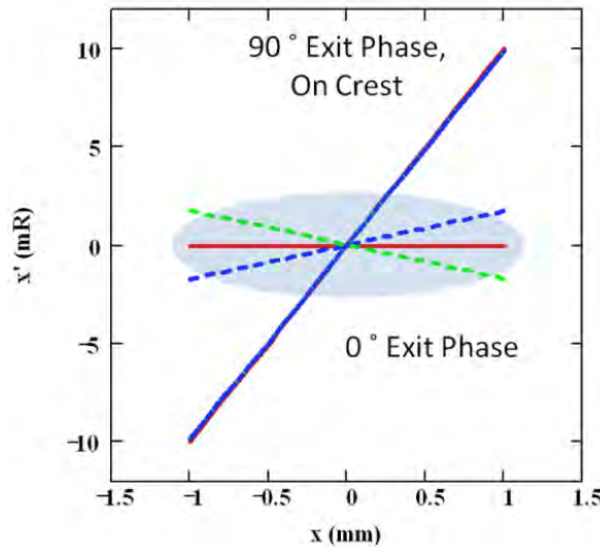
If we define the angular kick the beam gets at the iris exit in terms of the RF gun focal length

$$x' = \frac{x}{f_{RF}} \quad \boxed{f_{RF} = -\frac{2\beta \gamma mc^2}{eE_0 \sin \phi}} \quad \text{The beam out of the gun require a focusing force}$$

In numbers: $E_0 = 110 \text{ MV/m}$, $E_{gun} = 5 \text{ MeV}$ $\phi = 30 \text{ deg}$
 $f_{RF} \cong -18 \text{ cm}$

Linear and non-linear RF emittance

Phase dependent focal strength: electrons at various longitudinal positions along the bunch length, arriving at different phases at the gun exit, experience different kicks



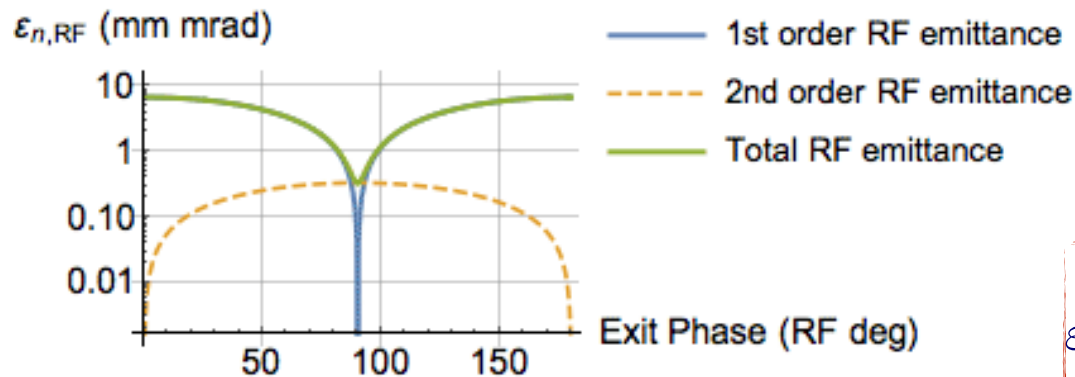
0 deg
 red solid: center slice
 blue dash: head slice
 green dash: tail slice
90° phase spaces
 all lie on the same diagonal line
The linear (first-order) emittance for an exit phase of 90° is zero, as shown by the diagonal line.

$$x' = \frac{x}{f_{RF}} \rightarrow \Delta x' = -\frac{d}{d\phi} \left(\frac{1}{f_{RF}} \right) \Delta x \Delta \phi$$

$$\sigma_{x'} = \frac{eE_0 \cos \phi}{2\gamma mc^2} \sigma_x \sigma_\phi$$

$$\epsilon_n = \beta\gamma \sqrt{\langle x^2 \rangle \langle x'^2 \rangle - \langle xx' \rangle^2} = \beta\gamma \sigma_x \sigma_{x'}$$

Correlation is neglected for exit phase far from 90 deg



$$\sigma_\phi = 4 \text{ deg} \Leftrightarrow 10 \text{ ps FWHM}$$

$$\sigma_x = 1 \text{ mm}, E_0 = 100 \text{ MV/m}$$

$$\epsilon_n^{RF} = \frac{eE_0}{2mc^2} \sigma_x^2 \sigma_\phi \sqrt{\cos^2 \phi + \frac{\sigma_\phi^2}{2} \sin^2 \phi}$$

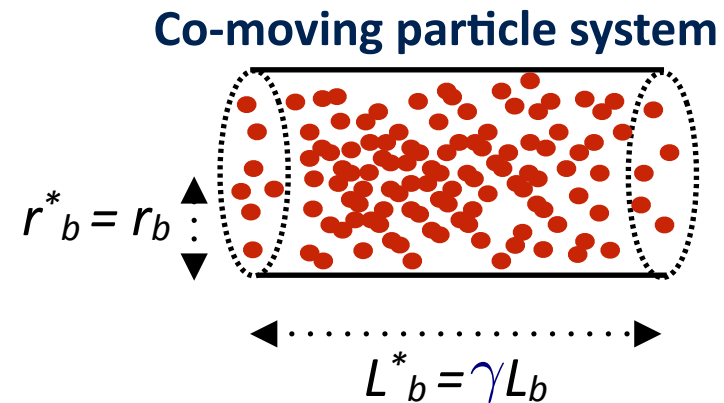
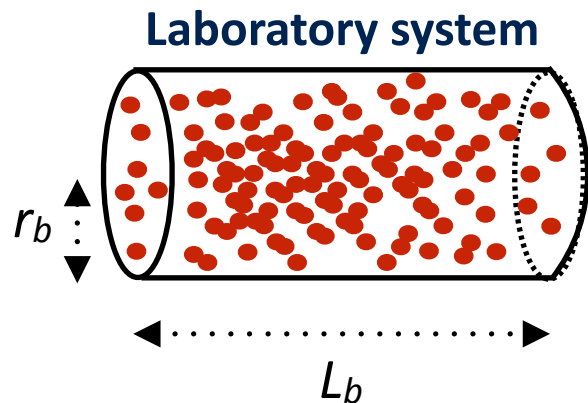
1st order RF emittance linear in σ_ϕ

Space Charge Effects

Space charge forces influence the beam dynamics and are one of the main performance limitations in high brightness photo-injectors

Let's consider first space charge forces in highly relativistic bunches

- Laboratory system: N relativistic electrons uniformly distributed in a cylinder with radius r_b and length L_b
- Co-moving particle coordinate system: electrons are at rest and a pure Coulomb field inside the bunch



$\gamma \gg 1$, $L_b^* \gg L_b$: the approximation of infinitely long cylindrical charge distribution is valid and the electric field has only a radial component

$$E_r^*(r) = -\frac{Ne}{2\pi\epsilon_0 L_b^*} \frac{r}{r_b^2} , r \leq r_b$$

$$E_r^*(r) = -\frac{Ne}{2\pi\epsilon_0 L_b^*} \frac{1}{r} , r \geq r_b$$

Space Charge Effects

Transforming back to the laboratory frame the radial component of the electric field yields to a radial electric field and an azimuthal magnetic field

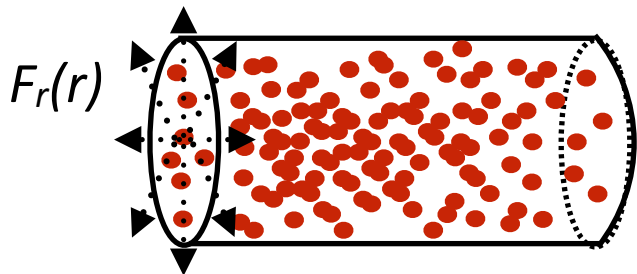
$$E_r(r) = \gamma E_r^*(r) = -\frac{Ne}{2\pi\epsilon_0 L_b} \frac{r}{r_b^2}$$

$$B_\phi = \frac{v}{c^2} E_r(r) , \quad r \leq r_b$$

The force a test electron inside the bunch experiences due to the E_r and B_{phi} field is determined through the Lorentz force

$$\vec{F} = -e(\vec{E} + \vec{v} \times \vec{B})$$

$$F_r(r) = \frac{Ne^2}{2\pi\epsilon_0 L_b} \frac{r}{r_b^2} \left(1 - \frac{v^2}{c^2}\right) = \frac{Ne^2}{2\pi\epsilon_0 L_b} \frac{r}{r_b^2} \frac{1}{\gamma^2}$$



The overall force points outwards and is then a defocusing force, which vanishes for $\gamma \rightarrow \infty$

Space Charge Dependence on Charge Density Distribution

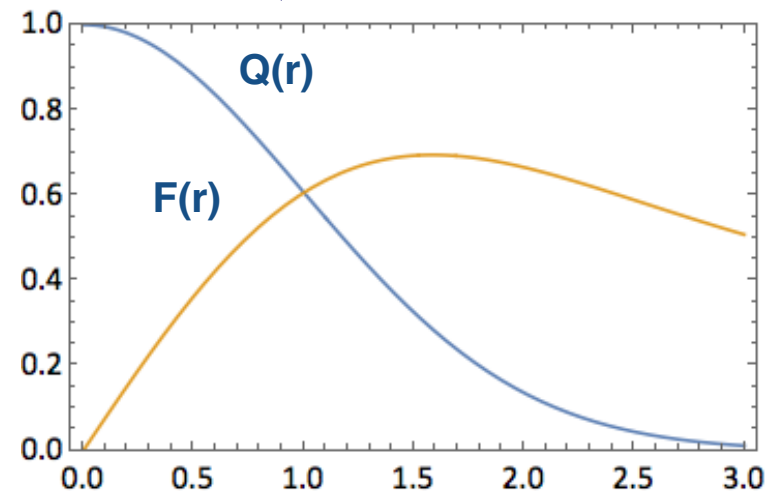
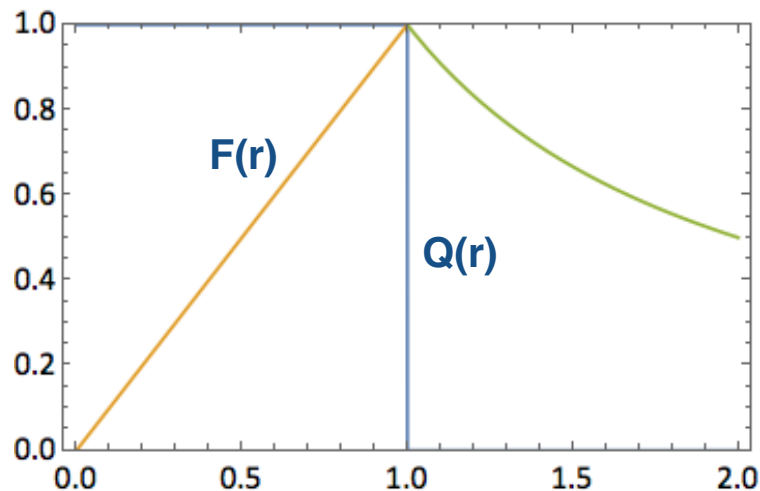
The repulsive space charge forces remain an unavoidable problem: is it possible to counteract these internal forces at least partially by applying an external focusing field?

For the cylindrical electron bunch with constant charge density, this is possible because the total space charge force depends linearly on the displacement r from the axis

$$F_r(r) = \frac{Ne^2}{2\pi\epsilon_0 L_b} \frac{r}{r_b^2} \frac{1}{\gamma^2}$$

What happens in case of a Gaussian transverse density distribution?

$$F_r(r) = \frac{Ne^2}{2\pi\epsilon_0 L_b r} \left[1 - e^{-\frac{r^2}{2\sigma^2}} \right] \frac{1}{\gamma^2}$$

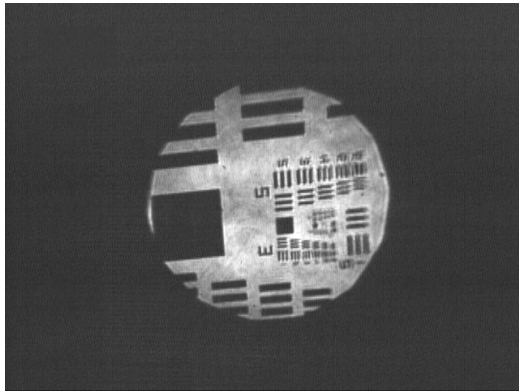


(Gun) Compensating Solenoid

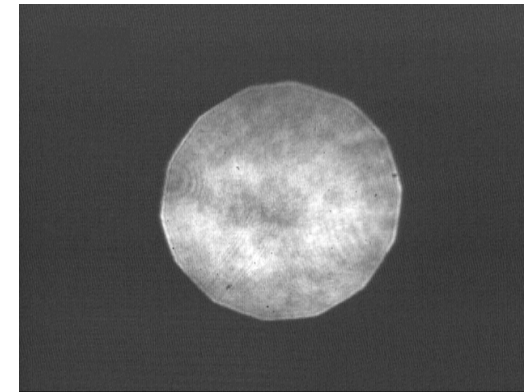
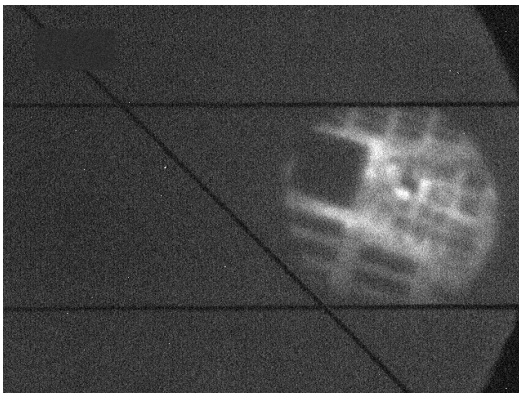
- The beam wants to diverge for 2 reasons
 - **Space charge**
 - The electron bunch coming off the cathode is very dense and wants to expand violently due to the electrostatic force
 - **Divergent RF Fields within the RF gun**
 - Anytime the electric field varies longitudinally there is a radial field
- The **solenoid focuses the low energy beam radially**

Multiple Role of the Gun Solenoid

- It cancels the strong negative RF lens effect
- it is **crucial for emittance compensation** by aligning the slices transversely along the bunch to minimize the projected emittance
- **Imaging the electron emission from the cathode** to have a good representation of the true QE map



Above: Laser cathode image of air force mask in laser room.
Below: Resulting electron beam.



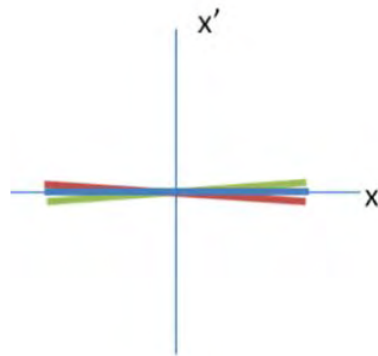
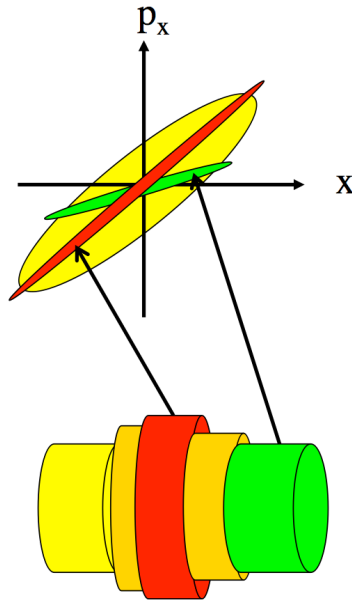
Above: Laser cathode image with mask removed showing smooth profile.
Below: Resulting electron beam showing hot spot of emission.



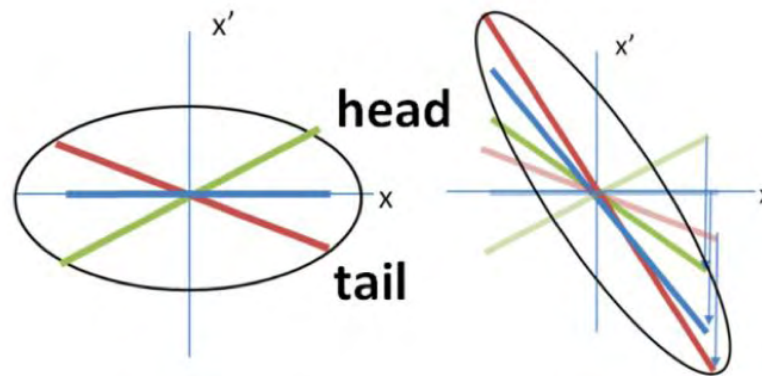
Courtesy of William S. Graves

Matching the low energy beam to the booster linac

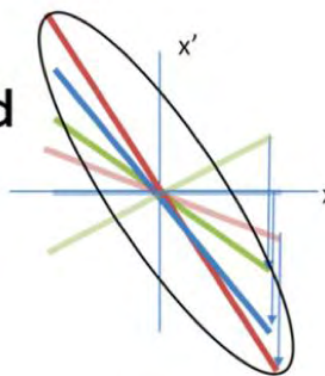
Emittance Oscillations are driven by space charge differential defocusing in core and tails of the beam



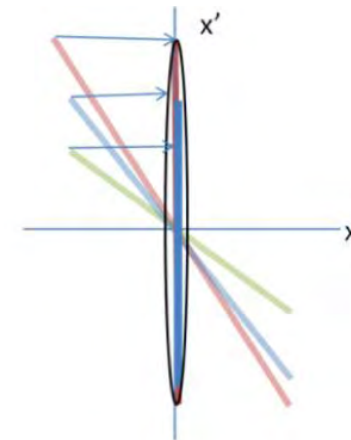
Cathode



After space charge kick



After solenoid lens

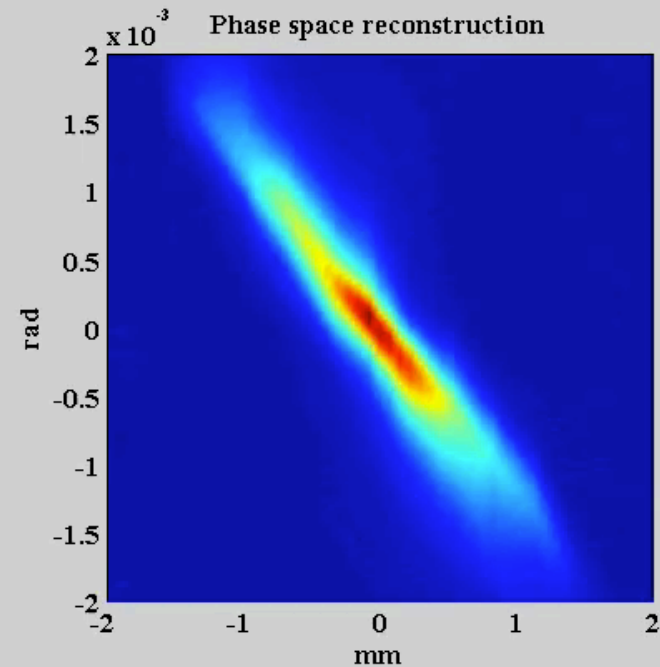
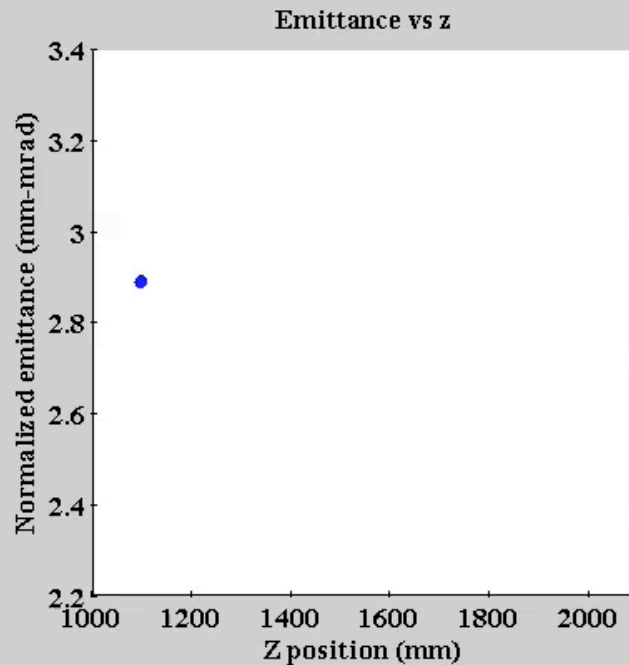


After drift, at beam waist

At or near the waist, the slices are once again lined up and the emittance goes through a minimum

Matching the low energy beam to the booster linac

Experimental evidence of emittance oscillations in the drift before the booster has been proved at the SPARC_LAB high brightness photo-injector

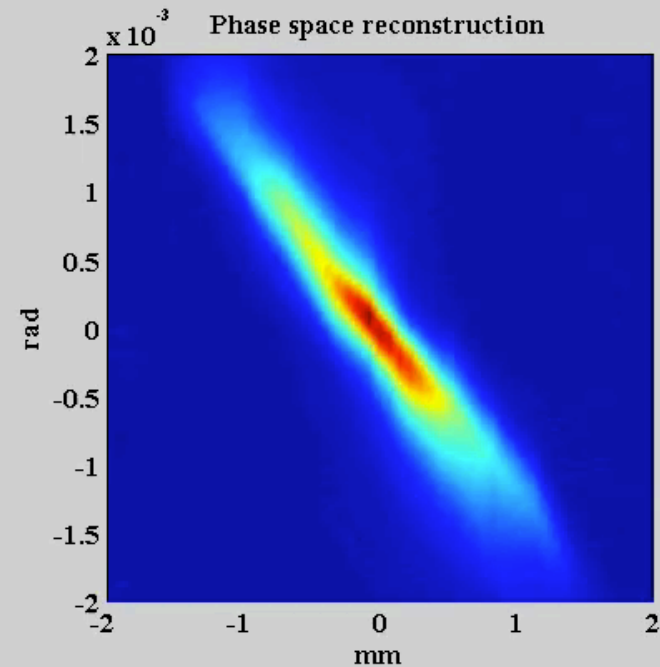
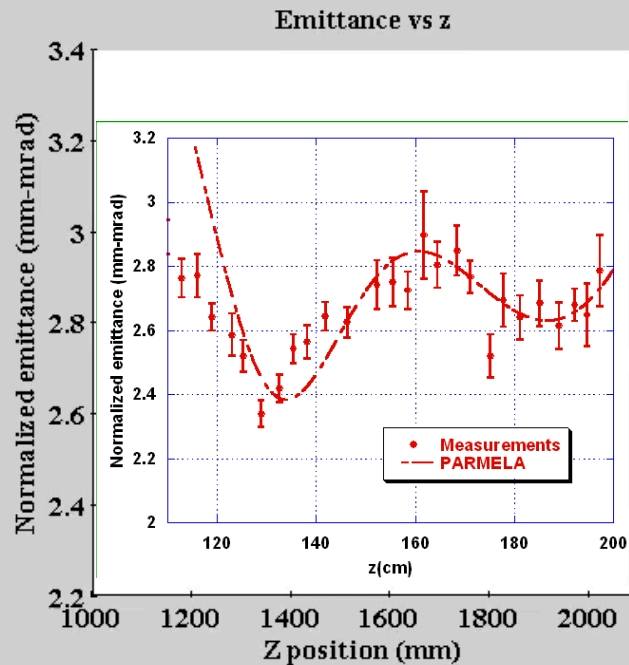


charge	0.5 nC
pulse length (FWHM)	5 ps
rise time	1.5 ps
rms spot size	0.45 mm
RF phase ($\varphi - \varphi_{\max}$)	+12°

M. Ferrario et al., *Direct Measurement of double emittance minimum in the SPARC high brightness photo-injector*
PRL **99**, 234801 (2007)

Matching the low energy beam to the booster linac

Experimental evidence of emittance oscillations in the drift before the booster has been proved at the SPARC_LAB high brightness photo-injector



charge	0.5 nC
pulse length (FWHM)	5 ps
rise time	1.5 ps
rms spot size	0.45 mm
RF phase ($\varphi - \varphi_{\max}$)	+12°

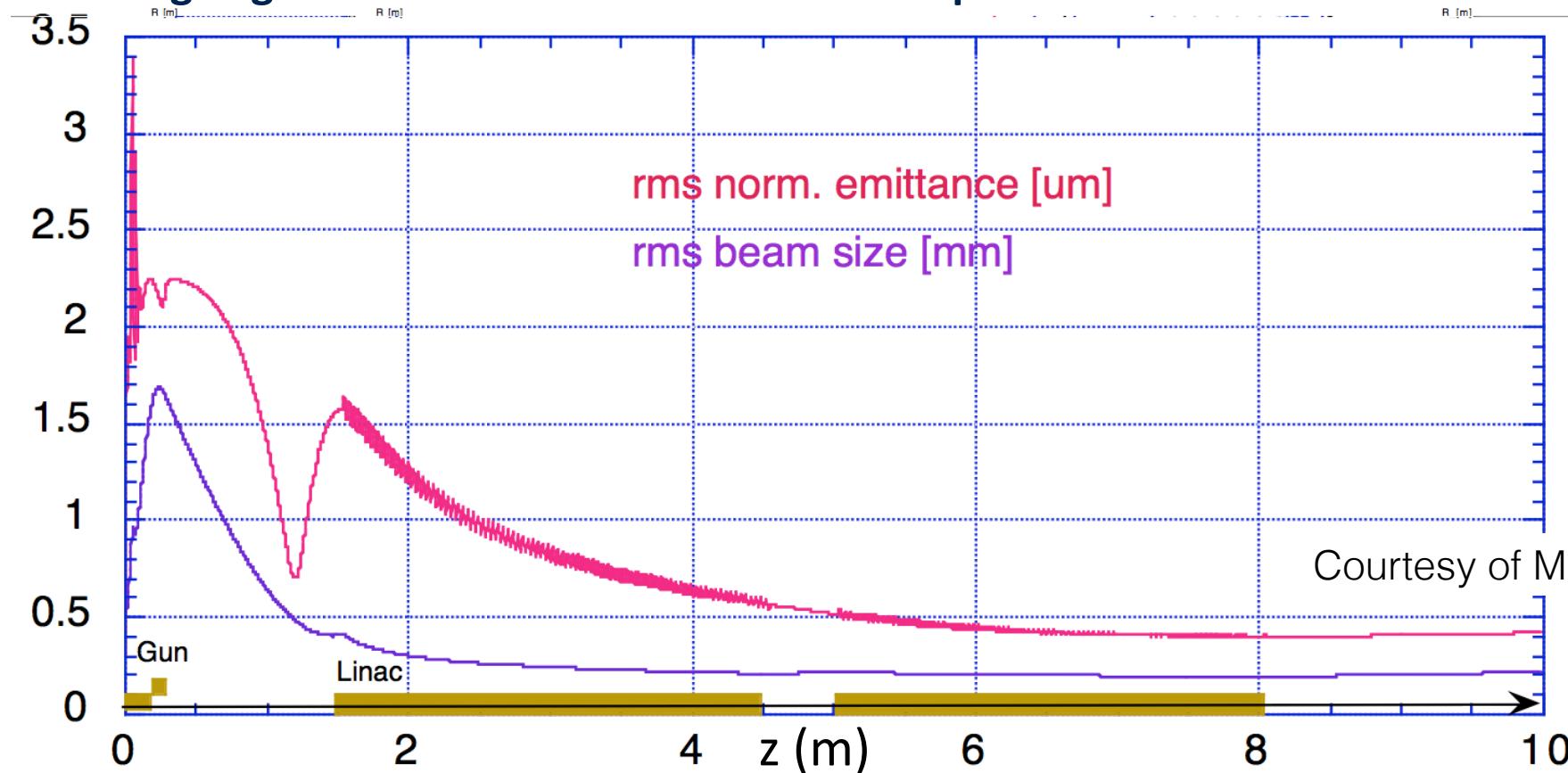
M. Ferrario et al., *Direct Measurement of double emittance minimum in the SPARC high brightness photo-injector*
PRL 99, 234801 (2007)

Matching the low energy beam to the booster linac

The beam needs to be matched into a high-gradient booster to damp the emittance oscillations

Matching condition: *Ferrario's working point* (M. Ferrario et al., "HOMDYN study for the LCLS RF photo-injector", SLAC-PUB-8400, LCLS-TN-00-04, LNF-00/004(P))

RF focusing aligns the slices and acceleration damps the emittance oscillations.



Courtesy of M. Ferrario

...

- To preserve brightness, it is desirable to accelerate the beam as quickly as possible, thus 'freezing-in' the space charge forces, before they can significantly dilute the phase space
 - RF gun
- Space charge can be controlled by reducing the beam charge density, especially in the cathode region where the beam energy is low
 - Larger transverse beam sizes at the cathode to reduce the density, but this increases the cathode intrinsic emittance
- Space charge can be also controlled by increasing the bunch length
 - Increase of longitudinal emittance
 - This in turn necessitates compression methods

Magnetic Compression

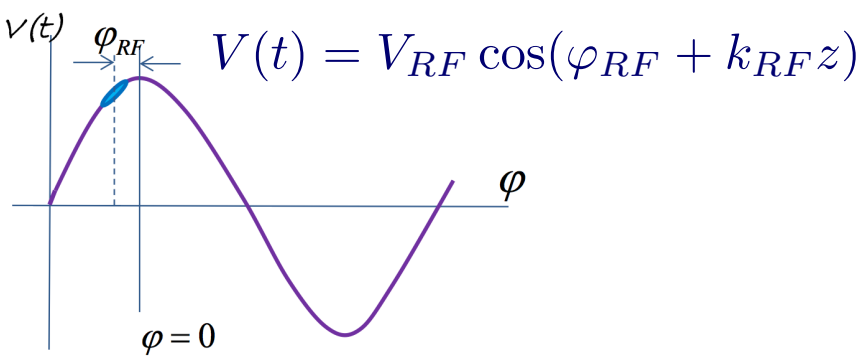
Picosecond electron bunches are produced in RF guns with peak current less than 100 A. Bunch compressors are used to compress the bunches to tens of femtoseconds to produce kA peak current at higher beam energy.



$$\begin{pmatrix} z_1 \\ \delta_1 \end{pmatrix} = \begin{pmatrix} 1 & 0 \\ R_{65} & R_{66} \end{pmatrix} \cdot \begin{pmatrix} z_0 \\ \delta_0 \end{pmatrix} = \begin{pmatrix} 1 & 0 \\ h_1 & \frac{E_{0c}}{E_{1c}} \end{pmatrix} \cdot \begin{pmatrix} z_0 \\ \delta_0 \end{pmatrix}$$

$$\begin{pmatrix} z_f \\ \delta_f \end{pmatrix} = \begin{pmatrix} 1 & R_{56} \\ 0 & 1 \end{pmatrix} \cdot \begin{pmatrix} z_i \\ \delta_i \end{pmatrix}$$

Accelerating voltage



Final position of an electron

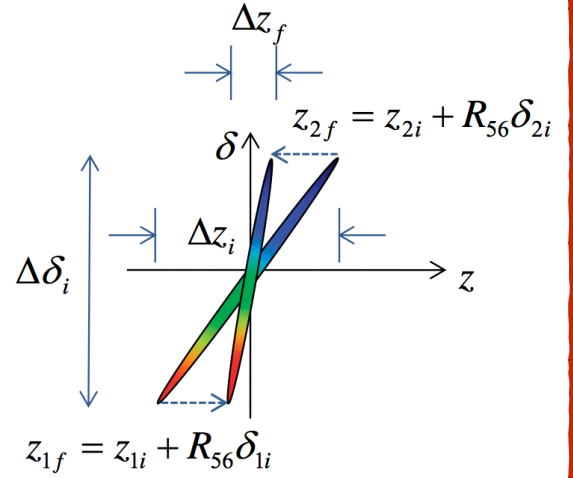
$$z_f = z_i + R_{56} \delta_i$$

change in bunch length

$$\Delta z_f = \Delta z_i + R_{56} \Delta \delta_i$$

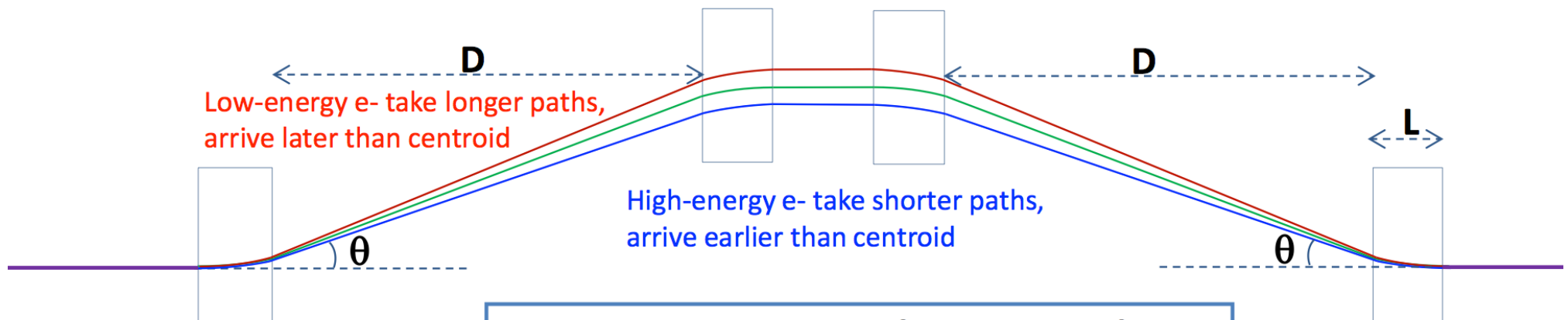
h_1 is the linear chirp induced by the cavity

$$h_1 = -\frac{e V_{RF} k_{RF}}{E_{1c}} \sin \varphi_{RF}$$

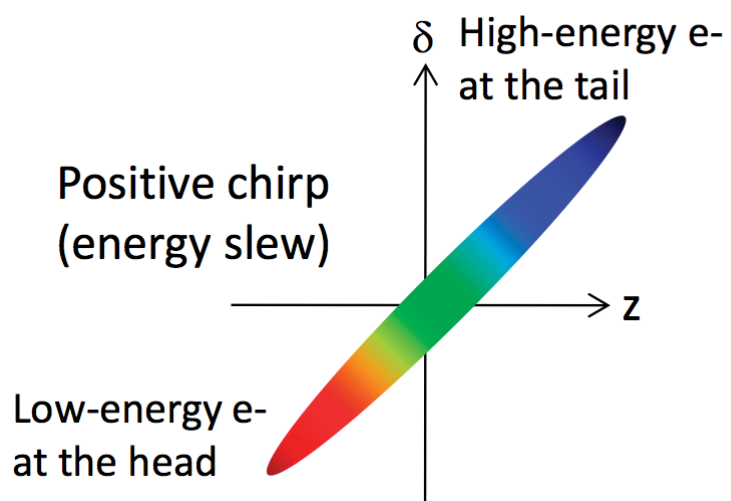


Chicane Compression

A chicane consists of four rectangular dipoles length L with the 1st and 2nd (also 3rd and 4th) separated by distance D . The distance between 2nd and 3rd does not contribute to R_{56} .



$$\Delta z = R_{56} \delta_1 + T_{566} \delta_1^2 + U_{5666} \delta_1^3 + \dots$$

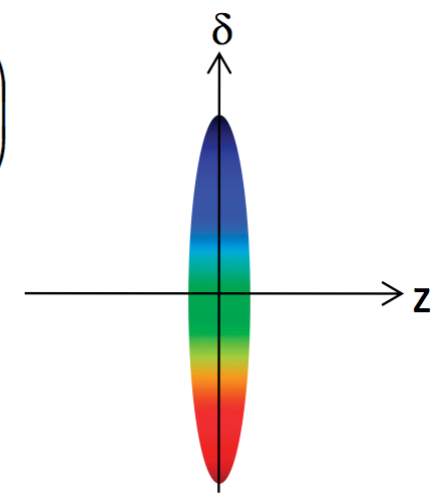


Chirped, uncompressed bunch

$$R_{56} \approx -\theta^2 \left(\frac{4}{3} L + 2D \right)$$

$$T_{566} \approx -\frac{3}{2} R_{56}$$

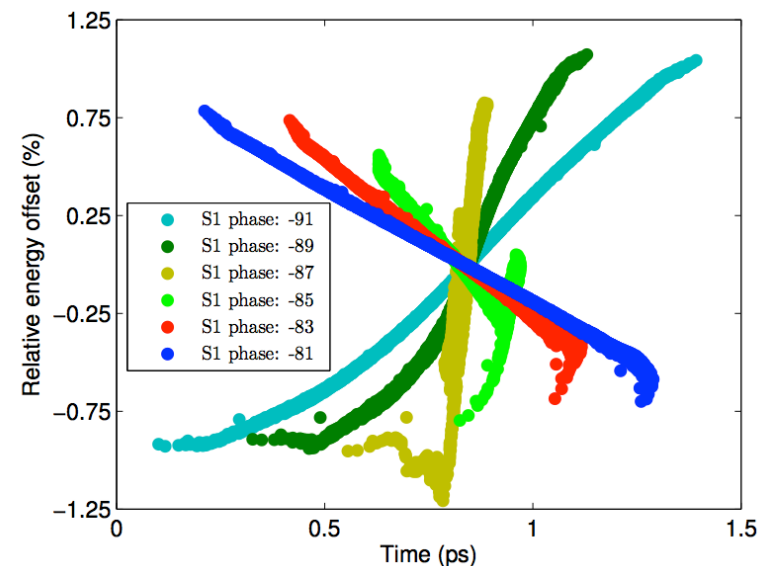
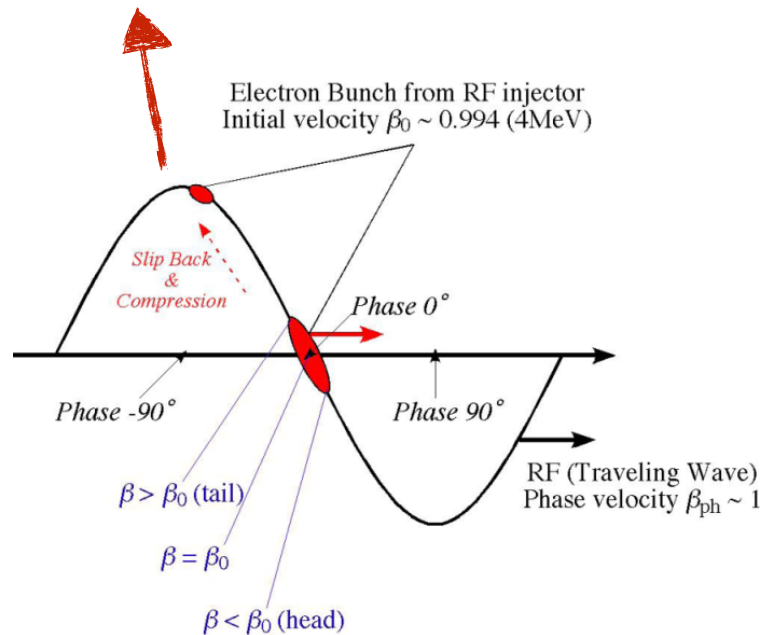
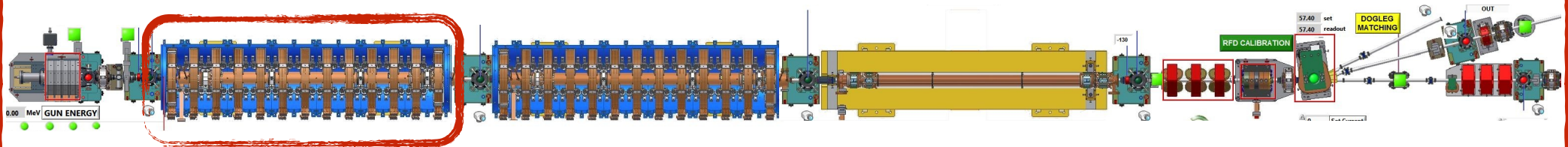
$$U_{5666} \approx 2R_{56}$$



Compressed bunch

RF Compression: Velocity Bunching

Sub-relativistic electrons ($\beta_c < 1$) injected into a traveling wave cavity at zero crossing move more slowly than the RF wave ($\beta_{RF} \sim 1$). The electron bunch slips back to an accelerating phase and becomes simultaneously accelerated and compressed. Rectilinear trajectories => non coherent synchrotron radiation emission

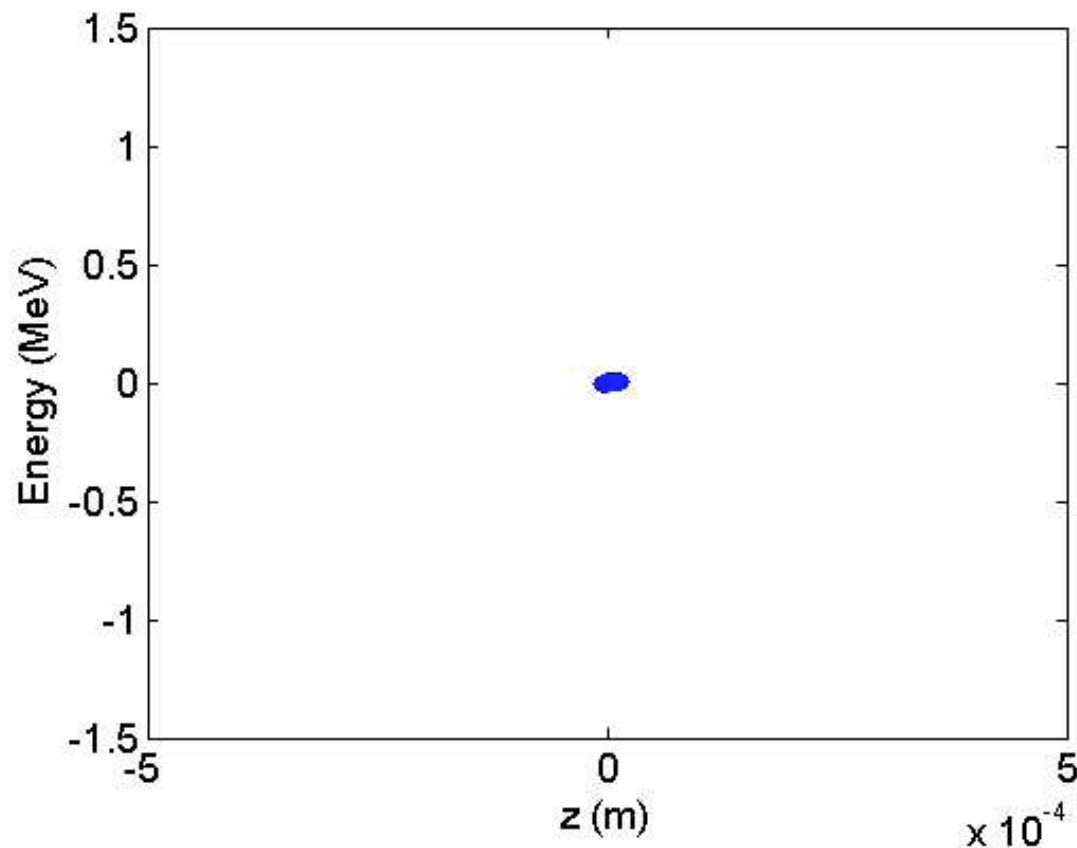


- **L. Serafini and M. Ferrario**, *Velocity Bunching in Photo-injectors*, Physics of, and Science with the X-Ray Free-Electron Laser, edited by S. Chattopadhyay et al. © 2001 American Institute of Physics
- **M. Ferrario et al.**, *Experimental Demonstration of Emittance Compensation with Velocity Bunching*, Phys. Rev. Lett. **104**, 054801 (2010)

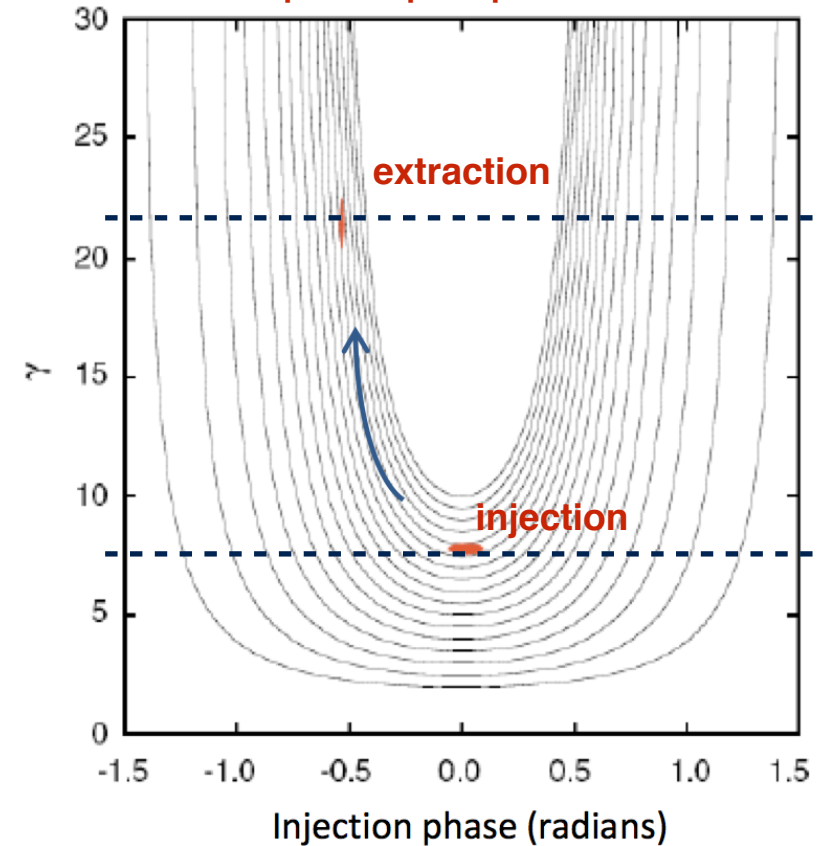
RF Compression: Velocity Bunching

An energy/phase correlation is imparted and removed smoothly, through phase slippage and acceleration, inside of the RF linac section.

The beam has no initial phase-energy correlation, injected at the zero-crossing of the wave, and ends with maximum energy spread and minimum phase extent



Zoom in of the phase space plot for a slow wave



Initial $\beta_c = 0.994$ at 4 MeV

Velocity Bunching

- It has been demonstrated to be well **integrated in emittance compensation schemes**
 - *M. Ferrario et al., Experimental Demonstration of Emittance Compensation with Velocity Bunching, Phys. Rev. Lett. **104**, 054801 (2010)*
- Compression happens along **rectilinear trajectories**
 - **No Coherent Synchrotron Radiation** which causes emittance dilution
- Compression and acceleration take place at the same time and within the same accelerating cavity
 - space charge force mitigation

Virtual Operation of a HB Photo-injector
The SPARC_LAB experience

The SPARC_LAB Test Facility

Beam energy	90 – 180 MeV
Bunch charge	50 – 700 pC
Rep. rate	10 Hz
ϵ_n	< 2 mm-mrad
σ_y	0.05% - 1%
Bunch length	<100 fs – 10 ps

FLAME laser transport line (Ti:Sa laser, 300 TW, < 30 fs)

Thomson back-scattering beamline

External injection beamline

Ti:Sa Laser

S-band RF gun

2 S-band structures

1 C-band structure

THz source

Test bench beamline

Cathode
Z=0
Z: beam propagation axis

r-PWFA experiments

Undulator beamline

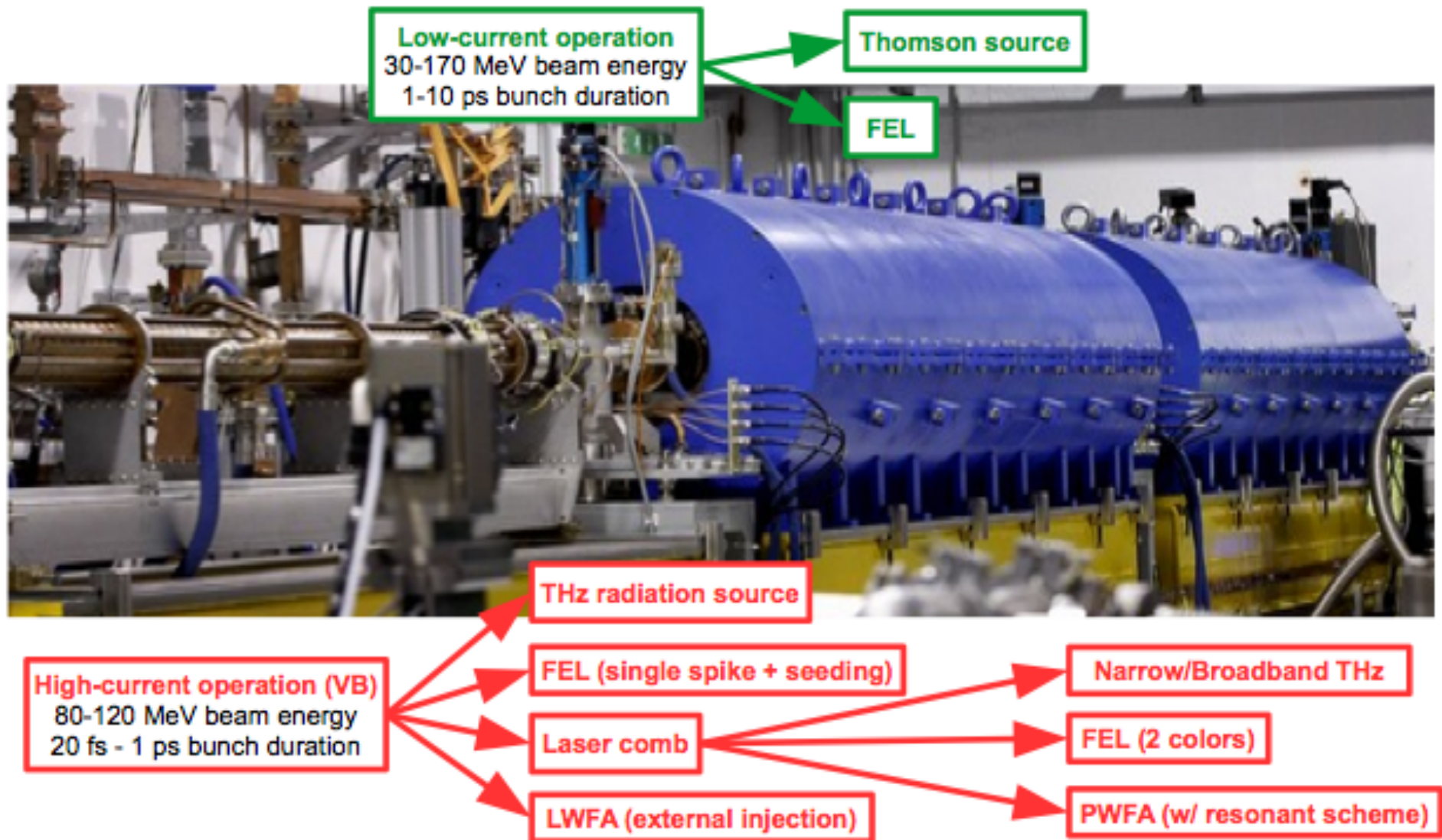
<http://www.lnf.infn.it/~chiadron/index.php>

Sources for Plasma Accelerators and Radiation Compton with Lasers And Beams

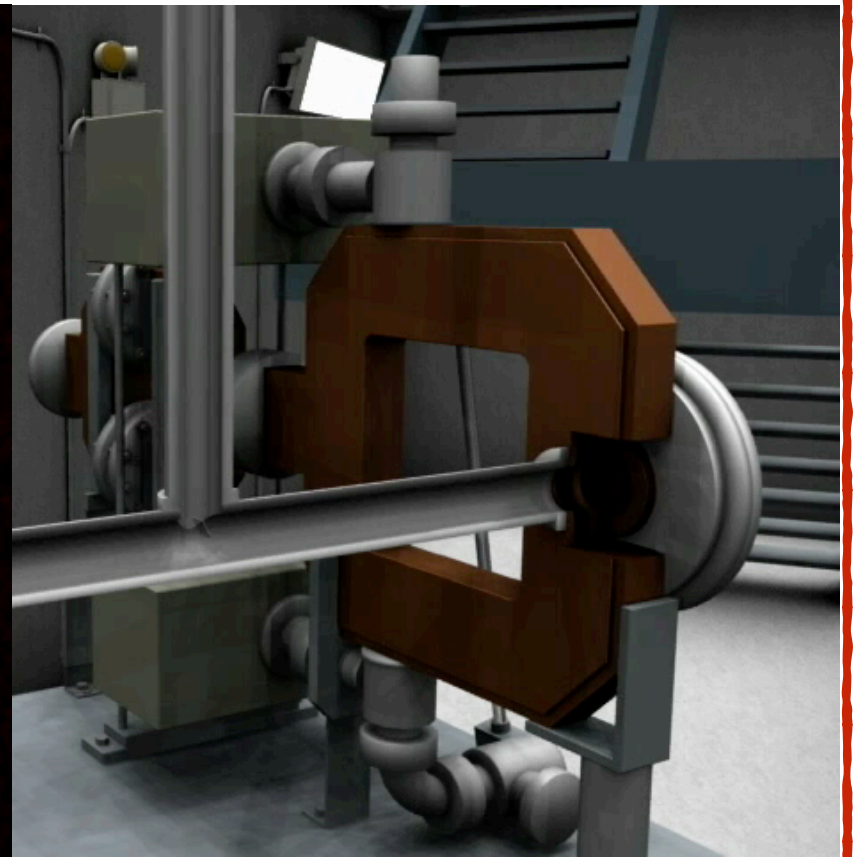
<https://www.google.it/maps/@41.8231995,12.6743967,3a,69.7y,130.68h,76.68t/data=!3m6!1e1!3m4!1sYyB35yaBMxJgQ92-wp3oYQ!2e0!7i13312!8i6656?hl=en>

The SPARC_LAB Test Facility

M. Ferrario et al., SPARC_LAB present and future, NIM B 309, 183–188 (2013)



Electron Emission

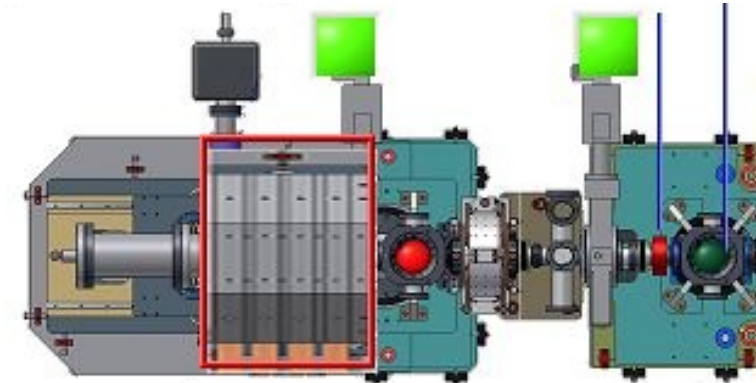
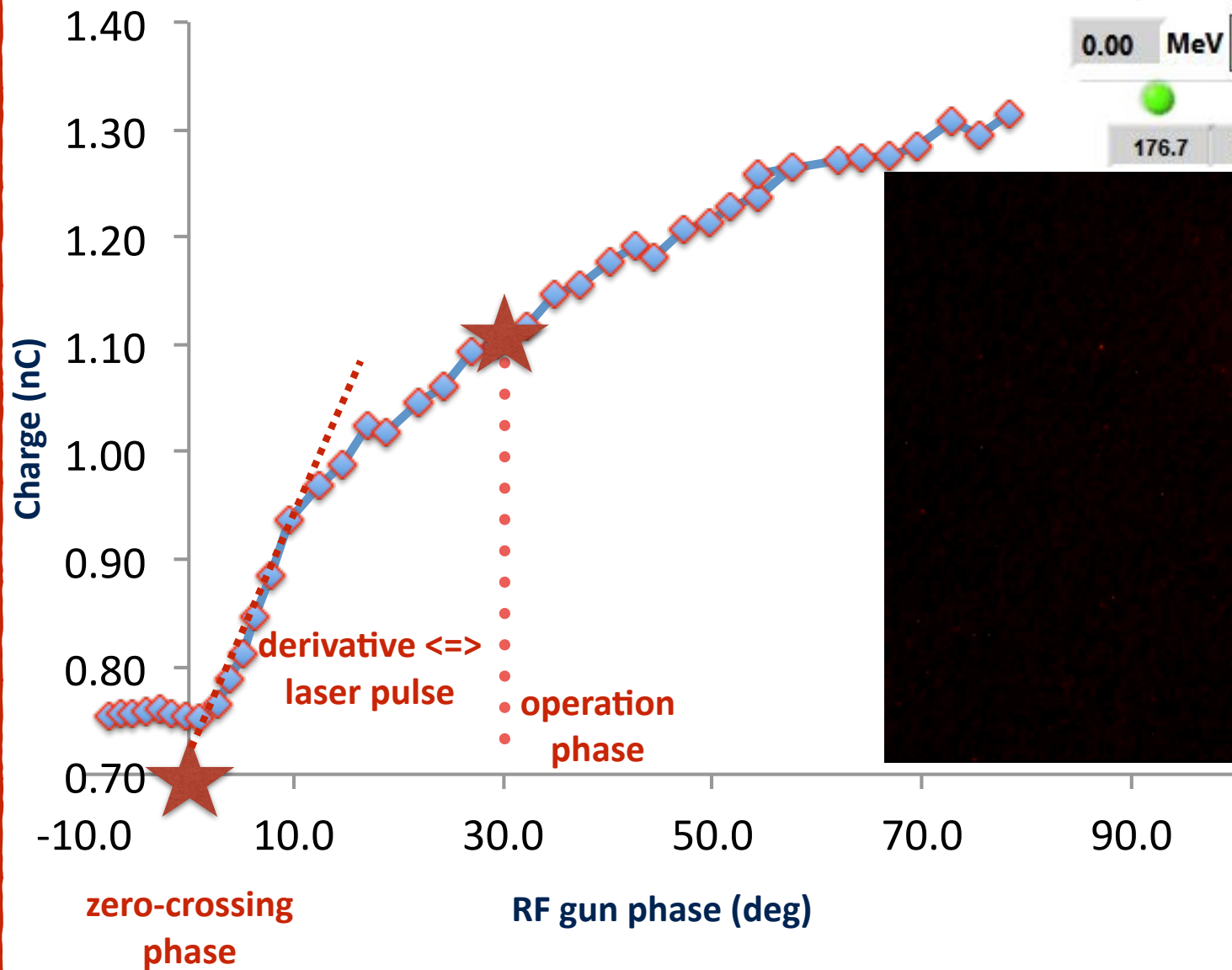


The extracted charge depends on the applied RF field and the RF gun phase

Radial expansion of the beam indicates the laser pulse is well aligned on the cathode, therefore the electron beam experience a radial force

The photo-cathode laser (266 nm) impinges on the copper cathode and electrons start to be extracted

Phase Scan

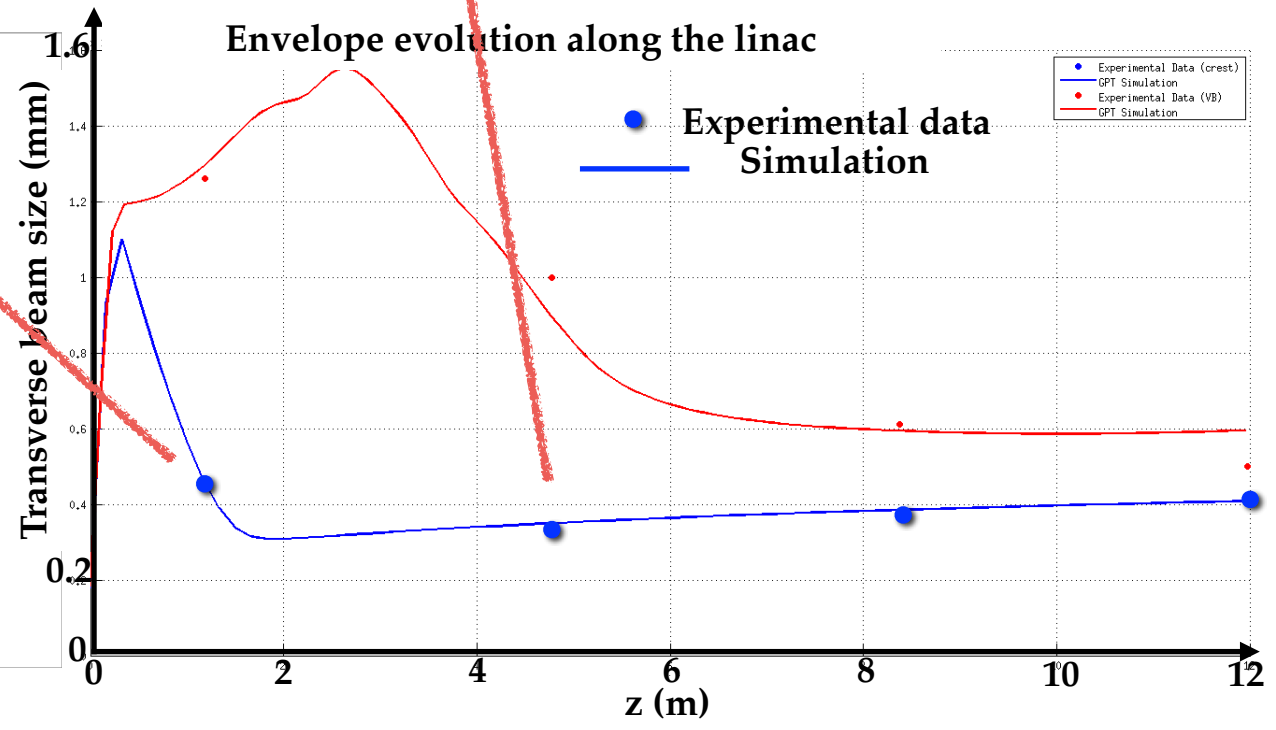
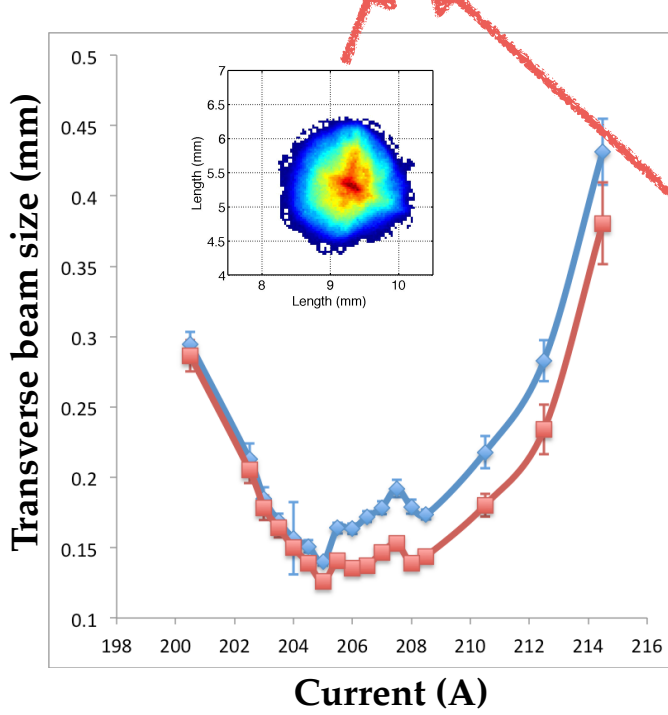
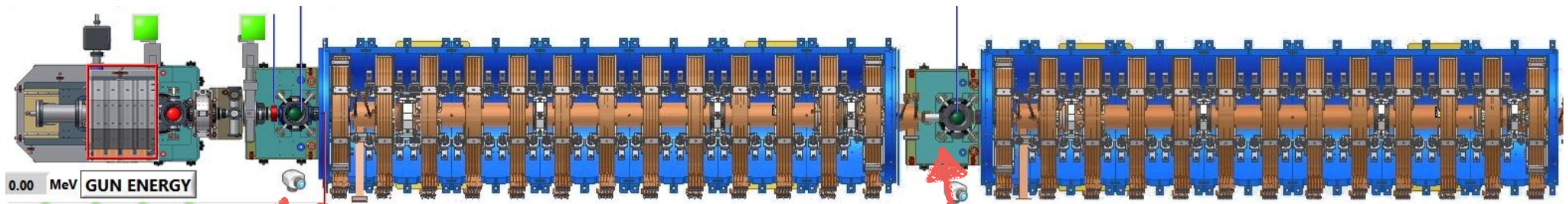


0.00 MeV GUN ENERGY

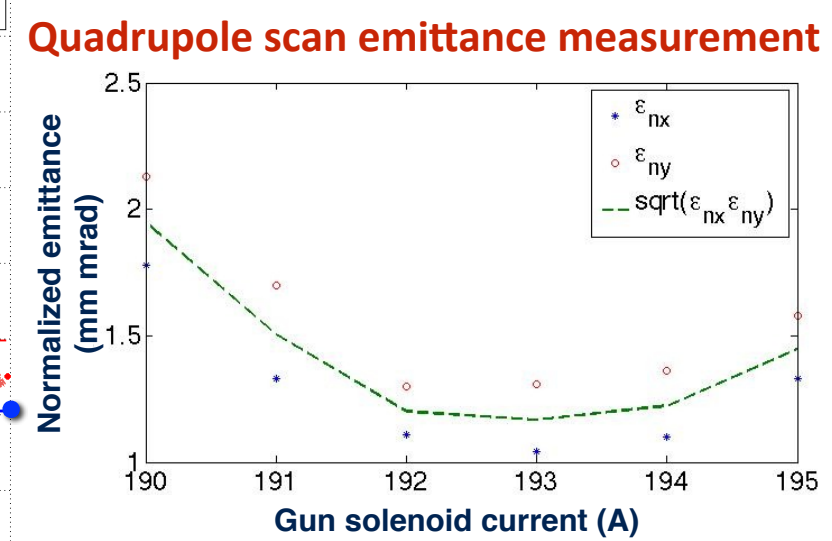
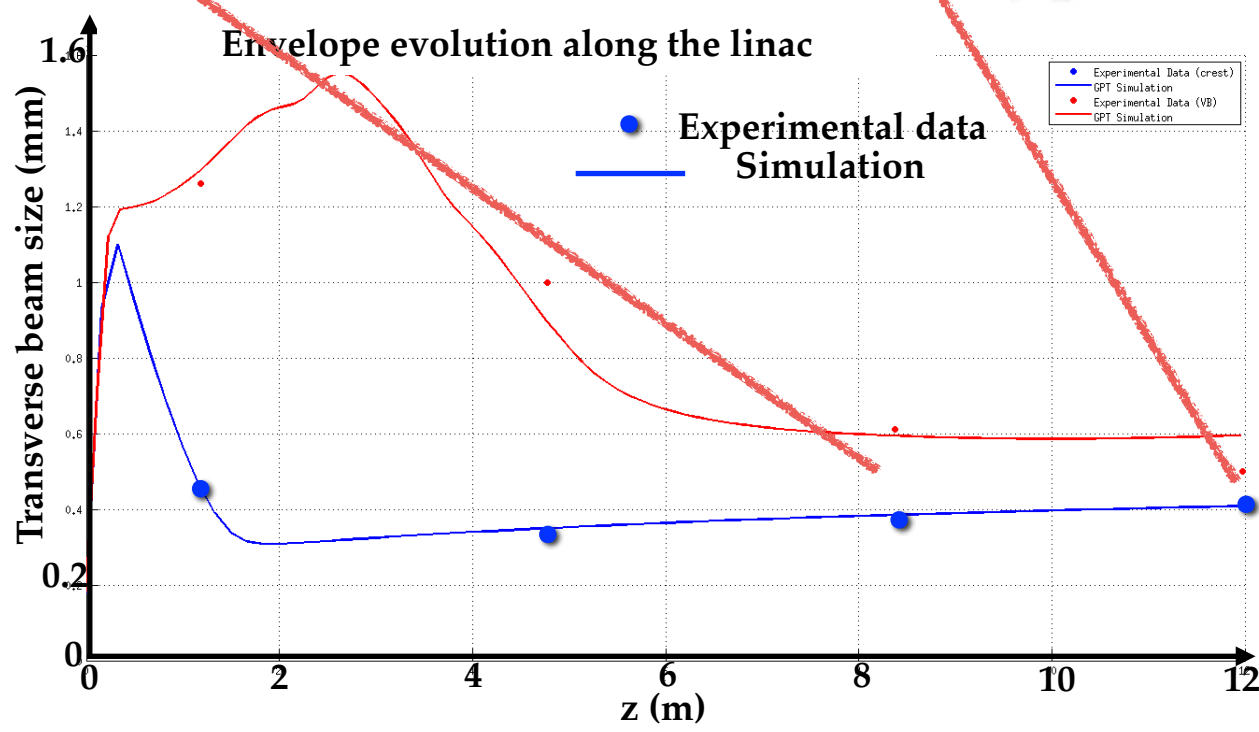
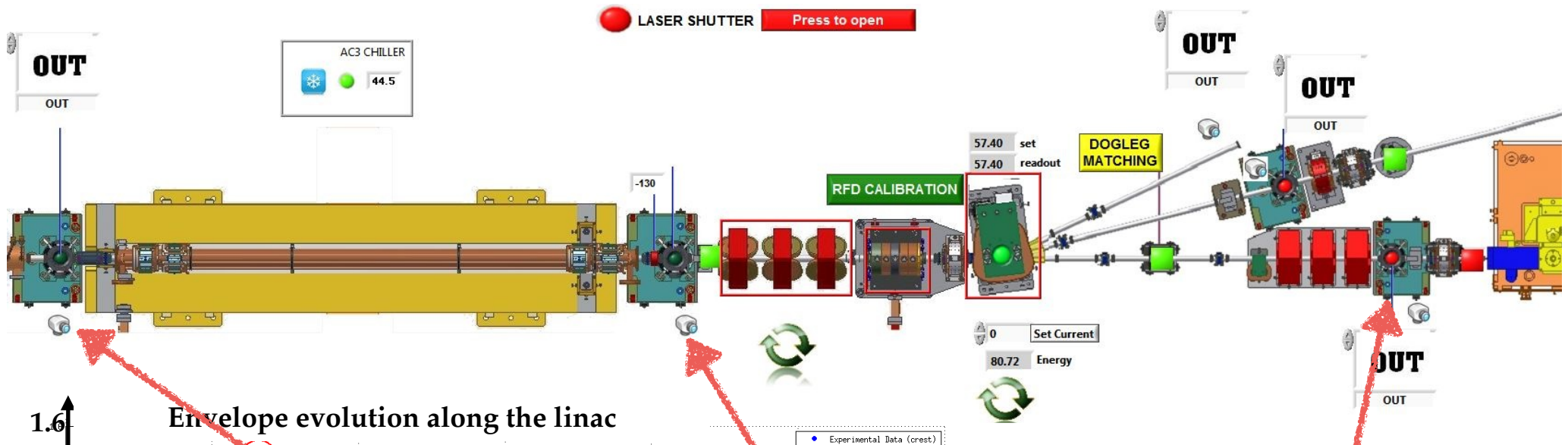
176.7	176.5	176.4	176.4
-------	-------	-------	-------



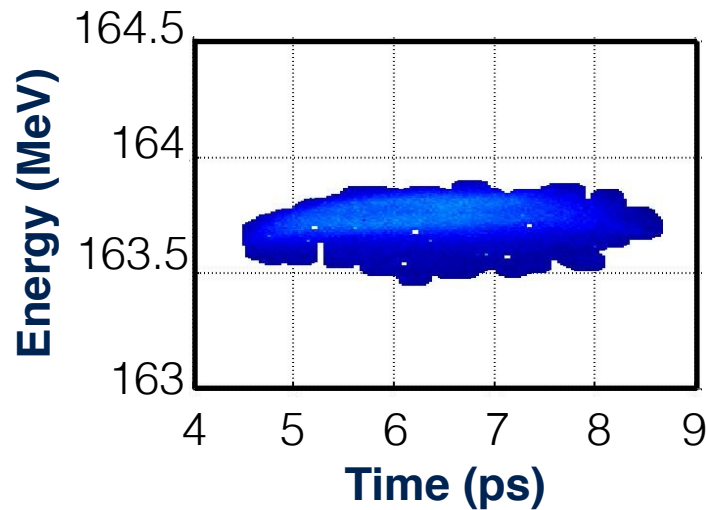
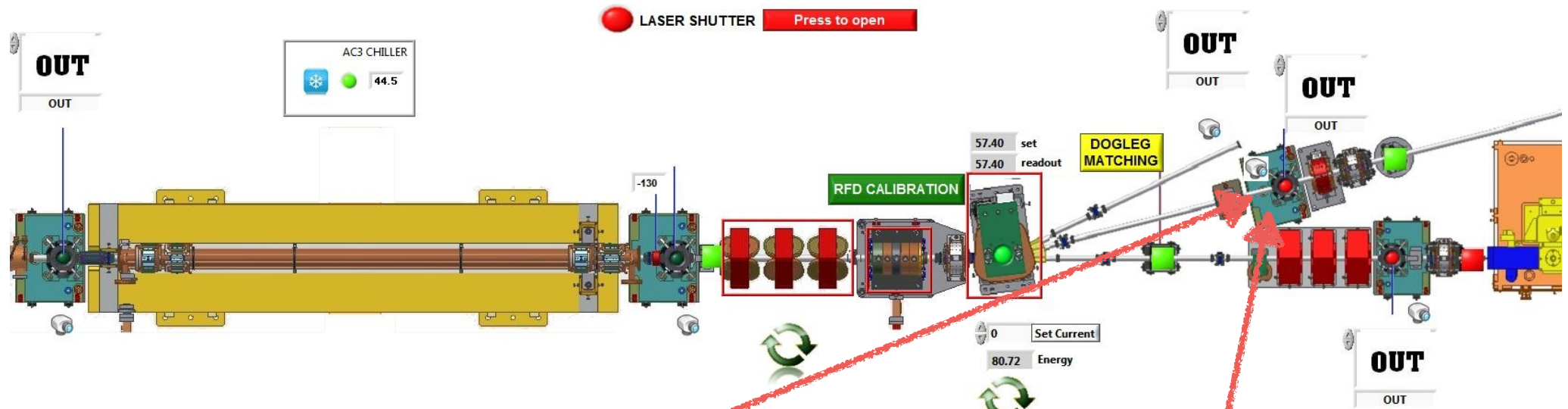
Beam Injection and "on crest" acceleration



On Crest Emittance Compensation

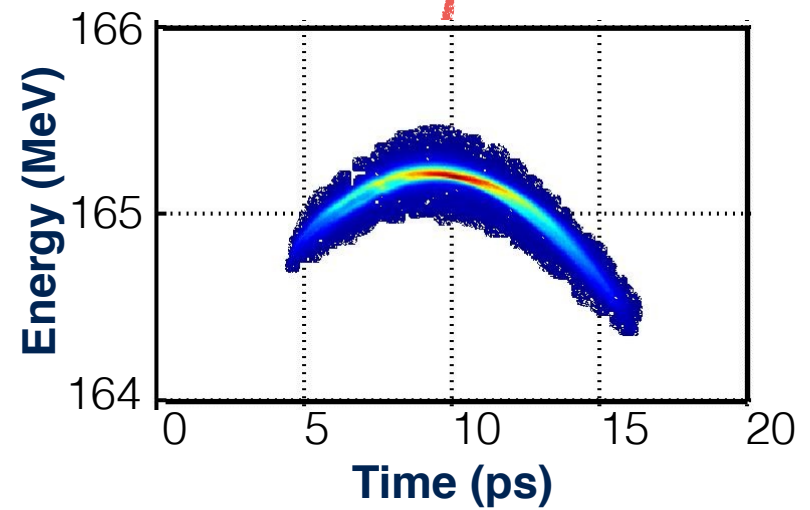


On Crest Energy Measurement



Sub-ps laser pulse

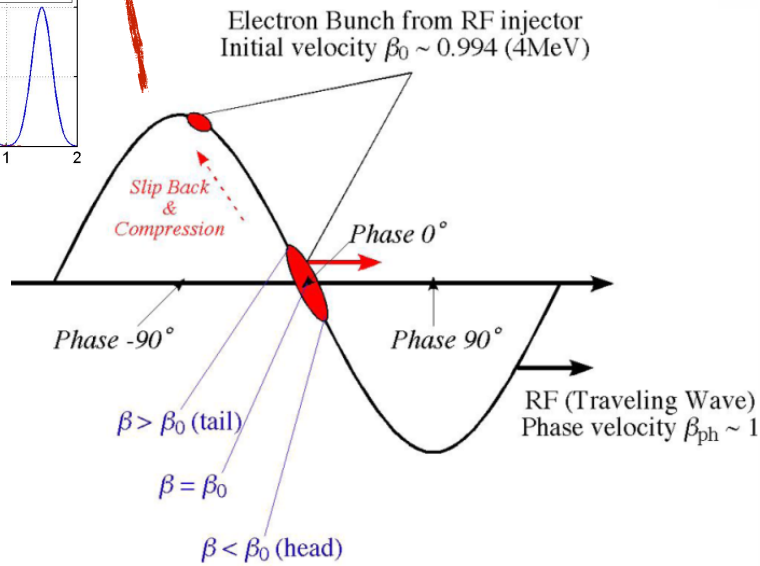
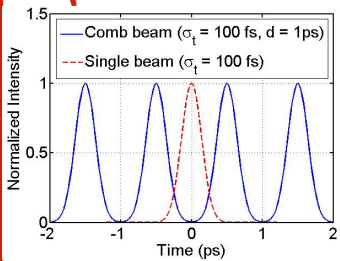
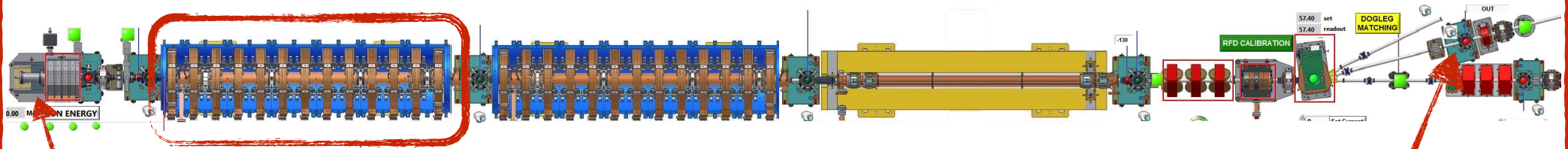
=> The electron beam does not experience RF non-linearities: **linear longitudinal phase space**



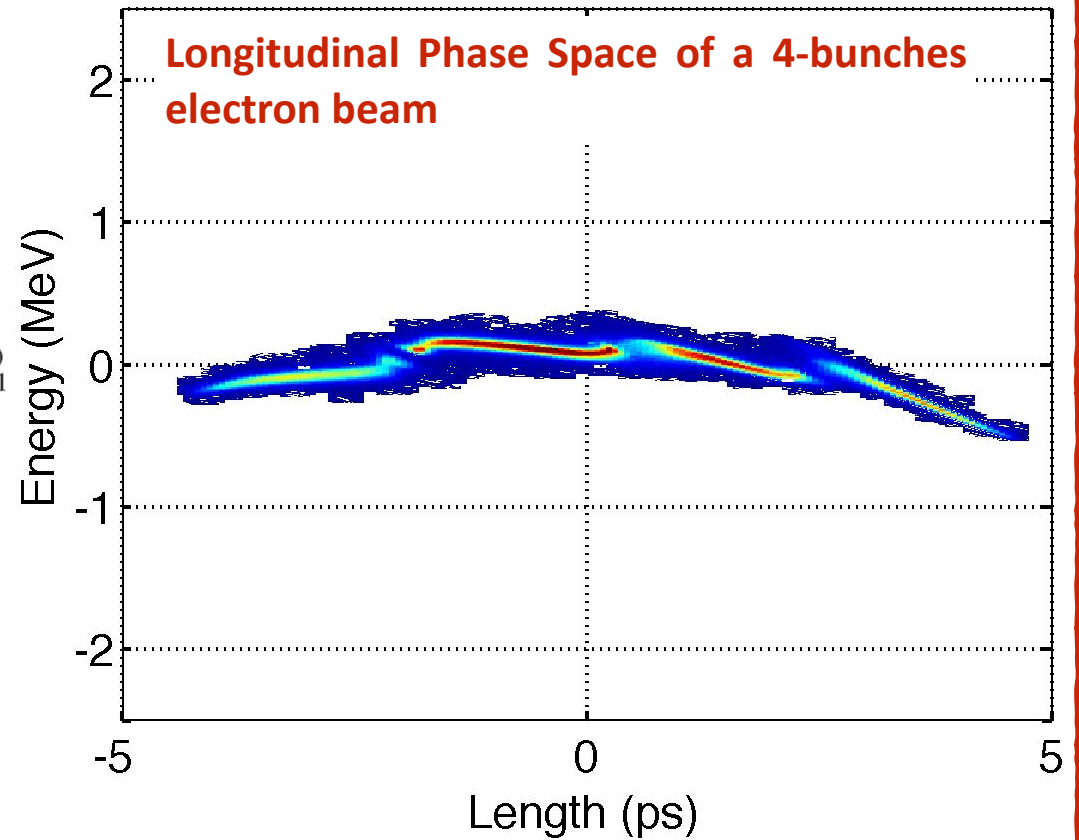
few ps laser pulse

=> The electron beam experiences RF non-linearities: **C-shape longitudinal phase space**

RF Compression

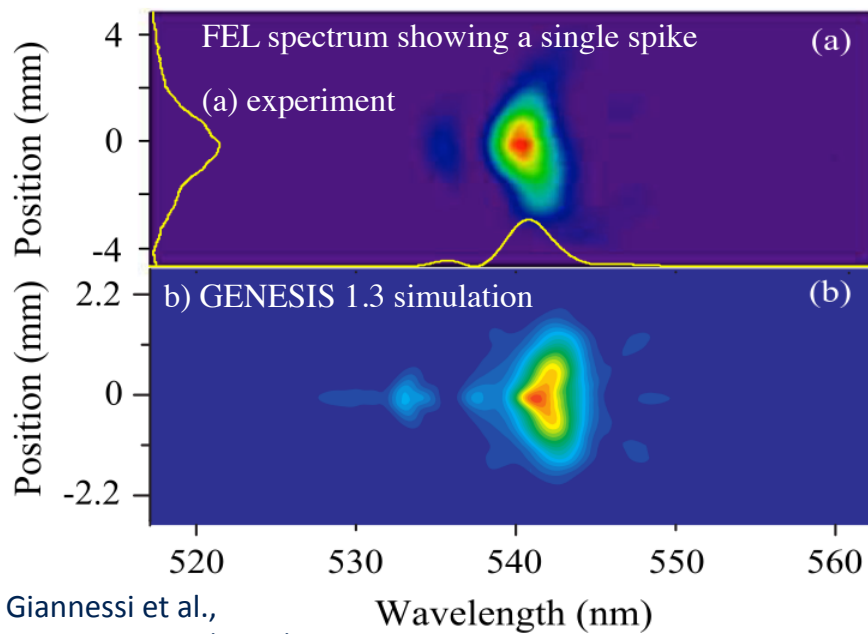
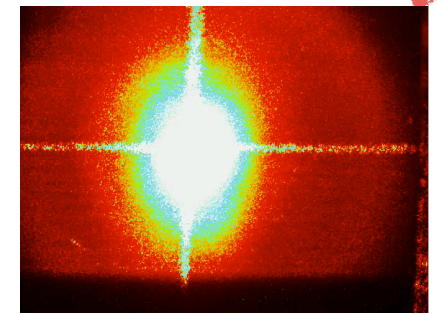
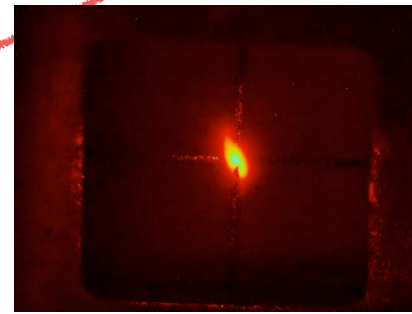
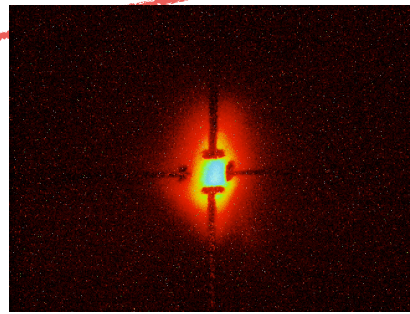
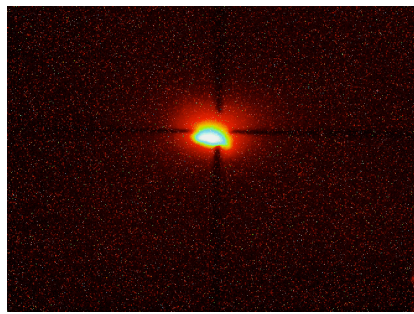
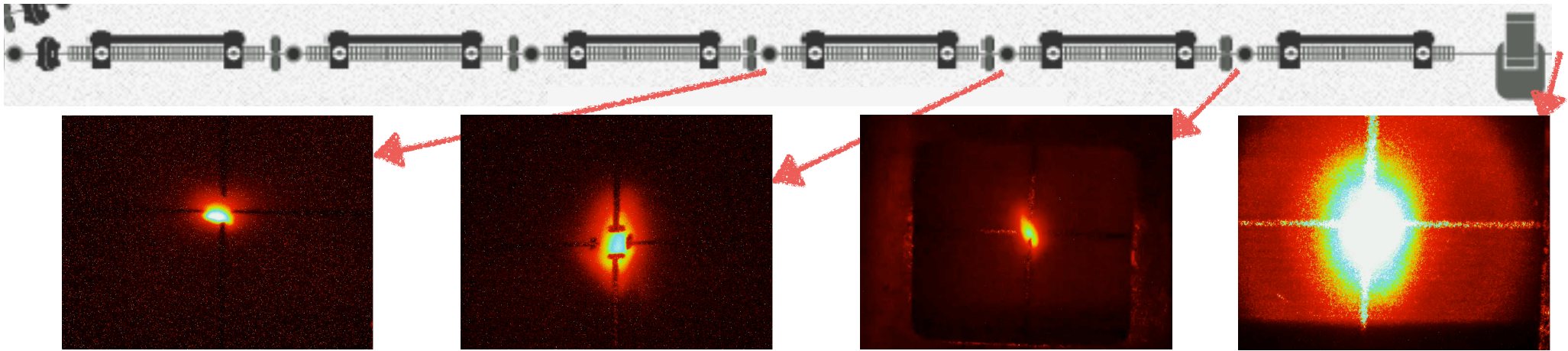


168 MeV, on crest

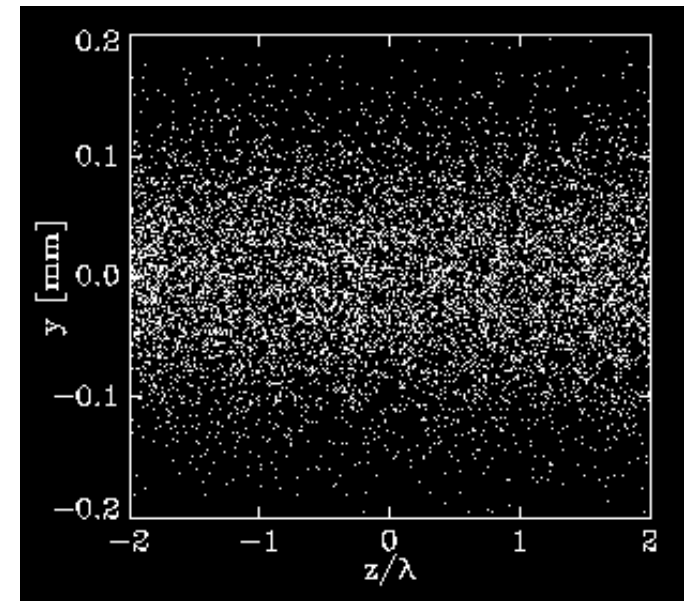


SASE FEL Radiation

Electron beam image on view screens while the gap is closing. Weak FEL radiation already after the third module. **Measurements at the SPARC_LAB Test Facility (INFN-LNF)**



S. Reiche, Simulation Code Genesis 1.3



Bibliography and Acknowledgment

Material from these lectures has been liberally taken from talks/papers/lectures/proceedings/notes from a large number of people which I acknowledge here together with a list of references

- Dowell, Rao, *An Engineering Guide To Photoinjectors*
- W. Anders, I. Bazarov, L. Cultrera et al., *An Engineering Guide to Photo-injector*, Editors D.H. Dowell and T. Rao, ISBN-13: 978-1481943222, ISBN-10: 1481943227
- <http://uspas.fnal.gov/materials/10MIT/MIT-High-Brightness.shtml>
- I. Bazarov et al., PRL **102**, 104801 (2009)
- K. Floettmann, *rf-induced beam dynamics in rf guns and accelerating cavities*, PRST AB 18, 064801 (2015)
- S. Di Mitri, M. Cornacchia, *Electron beam brightness in linac drivers for free-electron-lasers*, Physics Reports (2014), <http://dx.doi.org/10.1016/j.physrep.2014.01.005>
- P. Schmueser, M. Dohlus, J. Rossbach, *Ultraviolet and Soft X-rays Free Electron Lasers*, Springer (2008)
- T. P. Wangler, *RF Linear Accelerators*, Wiley-VCY
- http://uspas.fnal.gov/materials/14UNM/E_Bunch_Compression.pdf
- P. Musumeci's Lecture at <https://conf-slac.stanford.edu/sssep-2013/lectures>
- Papers of the SPARC_LAB collaboration